

THERMAL CONTACT RESISTANCE WITH
NON-UNIFORM INTERFACE PRESSURES

R. McMillan, Jr.

B.B. Mikic¹

Prepared for the National Aeronautics
and Space Administration
Grant No. NGR-22-009-(477)

November 1970

DSR PROJECT 72105

Engineering Projects Laboratory
Department of Mechanical Engineering
Massachusetts Institute of Technology
Cambridge, Massachusetts 02139

ABSTRACT

This work considers the effect of roughness and waviness on interfacial pressure distributions and interfacial contact resistance. It is shown that for moderate roughness the contour area could be substantially different from the contour area calculated using the Hertzian theory. The model for pressure calculation assumes plastic deformation of surface irregularities and elastic deformation of a spherically wavy base. The calculations of pressure distributions cover the range of parameters of practical interest. Experimental contact resistance values have been determined and are compared with theoretical predictions. It was calculated that contact conductance for wavy surfaces can be increased for certain ranges of parameters by making surfaces rough.

ACKNOWLEDGMENTS

This report was supported by the National Aeronautics and Space Administration under Grant No. NGR-22-009-(477).

TABLE OF CONTENTS

	Page
ABSTRACT	2
ACKNOWLEDGMENTS	3
TABLE OF CONTENTS	4
LIST OF FIGURES	6
NOMENCLATURE	7
1. INTRODUCTION	10
2. DESCRIPTION OF SURFACES	14
3. INTERFACE PRESSURE DISTRIBUTION	15
3.1 Governing Equations	15
3.2 Method of Solution	16
3.3 Pressure Distribution Curves	17
4. EXPERIMENTAL PROGRAM	19
4.1 Preparation of Specimens	19
4.2 Description of the Apparatus	20
4.3 Experimental Procedure	22
5. EXPERIMENTAL RESULTS AND DISCUSSIONS	23
6. CONCLUSIONS	24
BIBLIOGRAPHY	25
APPENDIX A - DERIVATION OF CONTACT RESISTANCE EQUATION	27
APPENDIX B - COMPUTER PROGRAMS	30
List of Fortran Variables Used in Programs	30
Program to Determine Dimensionless Pressure Distributions Between Rough and Wavy Surfaces	32
Program to Determine Contact Resistance Using Equation (5)	40

	Page
APPENDIX C - TABLES OF COORDINATES FOR PRESSURE DISTRIBUTIONS .	46
TABLE I - EXPERIMENTAL DATA	71
TABLE II - EXPERIMENTAL DATA	72
FIGURES	73

LIST OF FIGURES

Fig. 1	Definition of Contact Resistance
Fig. 2	Surface Contacts
Fig. 3	Surface Waviness
Fig. 4	Surface Geometry
Fig. 5	Typical Contact Area
Fig. 6	Plasticity Index vs. Dimensionless Force: Region of Significance for Roughness
Fig. 7 - 16	Dimensionless Pressure Distribution Curves
Fig. 17 - 19	Comparison of Hertzian and Rough-Sphere Pressure Distributions
Fig. 20	Radius Ratios: Smooth vs. Rough Spheres
Fig. 21	Surface-Profile Measuring Device
Fig. 22	Contact Resistance Apparatus
Fig. 23	Contact Conductance Results
Fig. 24	Non-Uniform Heat Transfer Coefficient
Fig. 25	Non-Uniform Heat Transfer Coefficient

NOMENCLATURE

a_H	Hertzian radius
\bar{a}_H	Dimensionless Hertzian radius, $a_H/(R_1\sigma)^{1/2}$
a_w	Contour radius
A	Area
A_{app}	Apparent contact area
A_c	Contour area
\bar{A}	$A/R_1\sigma$
b	Radius of heat channel
C.L.A.	Centerline average
C_n	Constant inside a summation
E_1, E_2	Moduli of elasticity of specimens in contact
\bar{E}	$\equiv \left(\frac{1 - \nu_1^2}{\pi E_1} + \frac{1 - \nu_2^2}{\pi E_2} \right)^{-1}$
F	Force
\bar{F}	$F/H\sigma R_1$
$f(\lambda)$	h/h_{av}
H	Microhardness of the softer of two materials in contact
h	Wave amplitude; Heat transfer coefficient
h_{av}	Average heat transfer coefficient
J_n	Bessel function of order n
k	Thermal conductivity--if two materials are in contact, $k = 2k_1k_2/(k_1 + k_2)$
P	Pressure
P_{av}	Average pressure

p_a	Average pressure over contour area
p_H	Hertzian pressure
p_L	Local pressure over Hertzian area
\bar{P}	P/H
Pl	Plasticity index $\equiv (\bar{E}/H) (\sigma/R_1)^{1/2}$
Q	Heat
$q/A, Q/A$	Heat flux over surface A
R	Thermal resistance; Radius of curvature
R_c	Constriction resistance
R_1	$R_1 R_2 / (R_1 + R_2)$
R_1, R_2	Radii of curvature of undeformed, spherically wavy surfaces
R_{MAC}	Macroscopic resistance term
r	Radial coordinate parallel to contact interface plane
\bar{r}	$r / (R_1 \sigma)^{1/2}$
r_1	A quarter-wavelength
r_o	Radius where pressure becomes zero
T_c	Local surface temperature
T_o	Ambient temperature
T_s	Extrapolated surface temperature
$w(r)$	Deformation of spherical object at point r
Y	Distance between the mean lines of specimen surfaces, measured in a direction perpendicular to the interface plane
\bar{Y}	Y/σ
y_i'	Slope of a surface profile at position i

z Vertical distance coordinate

Greek Letter Symbols

λ r/b

v_n Roots of $J_1(v_n) = 0$

v_1, v_2 Poisson's ratio of specimens in contact

ρ Distance between any point r and any elemental area
dA on the interfacial area

$\bar{\rho}$ $(\rho)/(R_1\sigma)^{1/2}$

σ Root mean square deviation of roughness heights--
 $\sigma = (\sigma_1^2 + \sigma_2^2)^{0.5}$ when two surfaces are in contact

$\text{Tan}\theta$ Mean absolute value of profile slopes-- $\text{Tan}\theta = (\text{Tan}_1^2\theta + \text{Tan}_2^2\theta)^{0.5}$
if two surfaces are in contact. More specifically,
 $\text{Tan}\theta_i \equiv \lim_{L \rightarrow \infty} \frac{1}{L} \int_0^L |y_1'| dx; \bar{i} = 1, 2, \dots$

ϕ_w Contact resistance factor

1. INTRODUCTION

Thermal resistances discussed in this work are assumed to occur in a vacuum environment, or in an environment where an interstitial fluid has a very low thermal conductivity. Thermal contact resistance is defined by

$$R = \frac{\Delta T}{q/A} \quad (1)$$

where (q/A) is the heat flux based on the apparent area, and ΔT is defined in Figure 1. Consider two pieces of smooth metal that are pressed together. As seen in Figure 2A, there is a finite number of contact points, A_c . The total actual contact area is often much smaller than the apparent area, A_{app} . Resistance to heat flow across such a joint is called contact resistance due to macroscopic constriction. The term "constriction" is used because heat-flow lines must squeeze together to pass through the contact area (see Figure 2B). Of course, the constriction would be present only in a vacuum, or where the interstitial fluid has a lower conductivity than the base material. If the surfaces are rough (Figure 2C), the true contact area will be even smaller than A_c . For this reason, A_c will from now on be referred to as a "contour area" rather than a "contact area." The additional area reduction due to roughness causes "microscopic constriction" of the heat-flow lines.

If $A_c = A_{app}$, only microscopic constriction is present, and the pressure distribution over the contour area is uniform. When both macroscopic and microscopic constriction are present, the pressure distribution is non-uniform, because of the clustering of contour areas at discreet locations.

Holm [6], Kragelski [7], Clausing [1], and Greenwood [3] developed equations for contact resistance under these conditions. They superimposed a microscopic constriction relation over another equation that applies to the macroscopic case. These relations, however, require a detailed knowledge of the contour area. Consider heat flow between two cylindrical solids whose channel radii are greater than the radius of their contour area (as in Figure 2B). In addition, let the surfaces originally be spherically wavy. There are three ways that one can model the heat transfer across the interface:

1. Assume constant temperature across the contour area;
2. Assume constant flux across the contour area; or
3. Assume that the heat flux through any point on the contour area is proportional to the microscopic conductance, which is in turn a function of the local pressure between the two surfaces.

In the first case, the maximum heat flux occurs at the outer rim of the contour area. For this reason, heat-flow lines that are outside the contour radius as $Z \rightarrow \infty$ must change their direction a minimal amount. The third case, however, places the maximum heat flux at the center of the contour area, making it necessary for the outer heat-flow lines to change direction substantially more. In the second case above, heat-flow is distributed in some intermediate fashion.

Resistance to heat flow is highest when the heat-flow lines must redistribute themselves to the greatest extent. For this reason, a contact resistance formula employing assumption (3) will be an upper bound for the actual contact resistance. Case (1) will consequently be a lower bound, and case (2) will fall somewhere in the middle.

A simple formula, e.g., Reference [2], predicts the macroscopic constriction resistance from the radius of the contour area:

$$R_{MAC} = \frac{\phi_w \pi b^2}{2k a_w} \quad (2)$$

where a_w is the contour radius, b is the channel radius, and k is the thermal conductivity. ϕ_w , the contact resistance factor, is given by

$$\phi = \left(1 - \frac{a_w}{b}\right)^{1.5}$$

where constant temperature is assumed and by

$$\phi = \frac{32}{3\pi^2} \left(1 - \frac{a_w}{b}\right)^{1.5}$$

for the case of constant flux. A similar resistance equation includes the effect of microscopic constriction resistance [9]:

$$R = \frac{b^2}{a_w^2} \frac{1}{h_c} + \frac{\phi_w \pi b^2}{2k a_w} \quad (3)$$

where

$$h_c = 1.45 \left(\frac{P_a}{H}\right)^{0.985} \frac{k \text{ Tan}\theta}{\sigma} \quad (4)$$

$\text{Tan}\theta$ is the mean absolute value of the profile slopes, and σ is the root-mean square deviation of roughness heights. P_a is the average pressure over the contour area, πa_w^2 .

We now have equations for models (1) and (2), assuming constant temperature or constant heat-flux across the contour area. Mikic [8] has developed an equation that falls into the third category, where contact resistance is a function of the contour area pressure distribution, $P(r)$:

$$R = 0.345 \frac{\sigma}{k \text{ Tan}\theta} \left[\int_0^1 \lambda \left(\frac{P}{H} \right)^{0.985} d\lambda \right]^{-1} + \frac{8b}{k} \sum_{n=1}^{\infty} \frac{\left[\int_0^1 \lambda \left(\frac{P}{P_{av}} \right)^{0.985} J_0(v_n \lambda) d\lambda \right]^2}{v_n J_0^2(v_n)} \quad (5)$$

b, σ , and $\text{Tan}\theta$ have been defined above. Hardness and thermal conductivity are denoted by H and k, respectively, and λ is the dimensionless radial coordinate $\lambda \equiv r/b$. J_n is the Bessel function of order n, and v_n are the roots of

$$J_1(v_n) = 0 .$$

P_{av} is the average pressure over the apparent area. A summary of the derivation of this equation appears in Appendix A. Knowledge of the interfacial pressure distribution is required for this equation. The Hertzian pressure distribution for a smooth sphere pressed against a rigid flat plane cannot, in general, be used as an approximation. Greenwood [4] has shown that in many instances the pressure distribution under a rough sphere is substantially different from the Hertzian approximation.

This work evaluates numerically the required pressure distribution curves for rough, wavy surfaces in contact. The curves are compiled in terms of convenient dimensionless parameters. In addition, experimental values of contact resistance are presented and compared with theoretical results.

The model used in this work assumes that microscopic surface irregularities are random and normally distributed, and their deformation is plastic. Deformation of the spherically wavy base surface is elastic.

2. DESCRIPTION OF SURFACES

The surfaces considered in this investigation are both wavy and rough. A surface is wavy if its profile has a finite radius of curvature along some finite length (see Figure 3). Roughness appears as a zig-zag pattern of surface heights superimposed over the waviness. The surfaces considered are assumed to have a Gaussian distribution of heights. It has been shown in Reference [2] that for the purpose of determining contact resistance, the parameters σ , $\text{Tan}\theta$, and R provide a sufficient description of the surfaces involved. σ is the root-mean-square deviation of roughness heights, and $\text{Tan}\theta$ is the absolute slope of these irregularities. In a wavy surface, R is the radius of curvature of a half-wave. A convenient way of finding R is by charting the surface profile and using the following equation (refer to Figure 3):

$$R = \frac{(\frac{1}{4} \text{ wavelength})^2}{2 (\text{wave amplitude})} = \frac{r_1^2}{2h} \quad , \quad (\text{for } \frac{h}{R} \ll 1) \quad . \quad (6)$$

A description of surface-profile measuring devices is given later on in this paper.

3. INTERFACE PRESSURE DISTRIBUTION

3.1 Governing Equations

The following equations determine the pressure distribution between two rough and wavy surfaces in contact under a load F:

$$P = \frac{H}{2} \text{ERFC} \left(\frac{Y}{\sqrt{2} \sigma} \right) \quad (7)$$

$$Y(r) = Y(0) + \frac{r^2 (R_1 + R_2)}{2 R_1 R_2} - \frac{2\pi}{E} \int P \, dr + \frac{1}{E} \iint_A \frac{P}{\rho} \, dA \quad (8)$$

$$F = \iint_A P \, dA . \quad (9)$$

Non-dimensional versions of these equations are:

$$\bar{P} = \frac{1}{2} \text{ERFC} \left(\frac{\bar{Y}}{\sqrt{2}} \right) \quad (7a)$$

$$\bar{Y}(F) = \bar{Y}(0) + \frac{1}{2} \bar{r}^2 - \frac{2\pi}{P\bar{l}} \int \bar{P} \, d\bar{r} + \frac{1}{P\bar{l}} \iint_{\bar{A}} \frac{\bar{P}}{\bar{\rho}} \, d\bar{A} \quad (8a)$$

$$\bar{F} = \iint_{\bar{A}} \bar{P} \, d\bar{A} . \quad (9a)$$

The variables in these equations are defined in the Nomenclature and Figures 4A, 4B, and 5.

Equations (7) and (7A) come from surface-height distribution theory and the assumption of plastic deformation of surface asperities [2]. Equations (8) and (8A) result from geometry and an assumed elastic deformation [11] as seen in Figure 4A. The final equation is a simple force balance which must be satisfied. The solution of these equations is described in Section 3.2.

The non-dimensional version of these equations results in (dimensionless) pressure vs. (dimensionless) radius curves that are functions of only two parameters, P_1 and \bar{F} . For practical purposes, the most useful plasticity index values range from 0.0 to 0.6. These values correspond to metals such as copper, aluminum, and stainless steel, with root-mean-square roughnesses from 20 micro-inches to 200 micro-inches, and whose wavy surfaces have radii of curvature between 25 inches to infinity.

3.2 Method of Solution

This section describes the technique used to find a pressure distribution employed by the contact resistance equation (Equation (5)). A pressure distribution is determined by an iterative procedure that refines a rough approximation until all three of the governing equations (7), (8), and (9) are simultaneously satisfied.

The Hertz solution for a smooth sphere pressed against a rigid flat wall [11] is taken as a first approximation for $Y(r)$. This $Y(r)$ is substituted into Equation (7) whose pressure is in turn placed in Equation (8) along with an arbitrary constant value of $Y(0)$. The new $Y(r)$ found from Equation (8) is then placed in Equation (7) and checked by (9) to determine if its load matches the actual load. At this point, $Y(0)$ is repeatedly modified until the pressures in (9) yield a force that is within 10 per cent of the correct load.

In some cases the calculated load will be lower than the actual load even when $Y(0) = 0$. Thus it would be impossible to reach the correct load by merely modifying $Y(0)$. When this condition exists, $Y(0)$ is immediately called zero, and the resultant pressures are sent directly to Equation (8).

Here the shape of the pressure distribution is changed until the correct load can be obtained. When the iteration process passes through Equations (7) and (8) twice in a row yielding approximately the same pressures (within 1 per cent), the computation is complete, and the desired pressure distribution is printed.

Computations were made using an I.B.M. 360. For the cases presented in this work, twenty-four radial increments have been used in the finite difference approximations. To be sure that twenty-four increments were sufficient, a test case was run at forty-eight increments also. Comparison of the two resulting pressure curves shows a maximum discrepancy of 5 per cent and an average discrepancy of less than 1 per cent. Based on the above, it was concluded that twenty-four increments yield sufficient accuracy.

In the calculation procedure, symmetry was imposed on the bulk elastic deflection by setting $w(0) = w(\Delta r)$ where $w(0)$ is the deflection at the center and $w(\Delta r)$ is the deflection at the first radial point. In this way, the slope of the deflection curve at the center line will be zero.

3.3 Pressure Distribution Curves

The Hertzian pressure distribution between two spherically wavy surfaces is given by

$$\bar{p} = \frac{1.5 \bar{F}}{\pi a_H^2} (1 - (\bar{r}/\bar{a}_H)^2)^{0.5} \quad (10)$$

where \bar{F} is the dimensionless applied load, and \bar{a}_H is the dimensionless Hertzian radius, $\bar{a}_H \equiv 1.333 (\bar{F}/P_1)^{1/3}$.

When a surface is rough, the pressure distribution may or may not differ significantly from the Hertzian solution. The region of P_1 vs. \bar{F}

plane where roughness is significant has been determined in this work and is presented in Figure 6. Roughness causes pressure distributions to differ significantly from Hertzian predictions in the following regions:

$$\bar{F} < 12.8 (P1)^{1.25}, 0 < P1 < .10 \quad (11)$$

$$\bar{F} < 11.7 (P1) - 0.25, .10 < P1 < .60 \quad (12)$$

Even outside of these regions, edge effects will cause the contour radius to be greater than the Hertzian radius.

Dimensionless pressure curves for the region defined above appear in Figures 7-16. Coordinates for these and other pressure curves are listed in Appendix C. Pressure curves close to the transition line in Figure 6 closely resemble Hertzian shapes, whereas far below this line, curves are much flatter. Figures 17-19 illustrate this by depicting pressure curves at extreme values of \bar{F} along with the associated Hertzian pressures. In each of these pictures, the curve with the higher maximum is the Hertzian pressure (p_H).

Let r_o be defined as the radial position where the pressure drops to zero. r_o is therefore the contour radius and is available from the enclosed pressure distribution solutions. The ratio of r_o over the Hertzian radius (a_H) becomes less as the applied load is increased. r_o/a_H is plotted as a function of $P1$ and \bar{F} in Figure 20. r_o/a_H approaches a constant value greater than one as \bar{F} values leave the region described by Equations (11) and (12). Outside this region, r_o should probably be used instead of a_H as the contour radius in Equations (2) and (3), whereas the Hertzian pressure distribution is in this case acceptable for Equation (5).

The r_o/a_H curves in Figure 20 are obtained from values of r_o which are read directly from Figures 8-16. There is some subjective interpretation as to where the pressure actually reaches zero. The behavior of the $P_1 = .1$ curve should be accepted with caution because (as seen in Figure 8) only three r_o values were used to construct that curve.

4. EXPERIMENTAL PROGRAM

4.1 Preparation of Specimens

Experiments are performed with solid circular cylinders 1-1/2 inches long and 1 inch in diameter. The specimens are cut from stainless steel 303 bar-stock. Four holes (size 55 drill) are drilled to the centerline of each specimen so that thermocouples can be inserted for measurement of the axial temperature drop. The first hole is 1/4 inch from the interface, and the rest of the holes are 3/8 inch apart.

The contact resistance interface surfaces are lapped nominally flat. Waviness is created by the following method: A specimen is rotated in a lathe while a hard rubber block is used to press an abrasive (emery paper or diamond paste) against the test surface. The velocity distribution of the abrasive relative to the interface surface causes wear to be an increasing function of radius. In this way, the longer the abrasive is held in contact, the more convex the specimen becomes.

After the degree of waviness has been measured by a surface profilometer, the surface is blasted with glass beads to provide a desired roughness.

Waviness measurements are taken using a device specially built to accommodate the 1-inch diameter, 1-1/2-inch long specimens used in contact resistance experiments (see Figure 21). This device consists of a specimen holder that slides slowly beneath a diamond stylus that is connected to the core of a linear variable differential transformer. As the specimen passes underneath the stylus, the stylus moves up and down to follow the specimen surface. The profile shape is traced out on a Sanborn 150 recorder. This profilometer is capable of magnifying the vertical

deflection by a factor of five hundred. A detailed description of this device may be found in Reference [5].

Roughness is measured on a Taylor-Hobson Talysurf IV. The "Talysurf" provides a profile chart and a direct reading of the centerline average (C.L.A.). The root-mean-square roughness (σ) can be determined by the following relation:

$$\sigma = [\text{C.L.A.}] (\pi/2)^{0.5} \cong 1.25 [\text{C.L.A.}] \quad (13)$$

The absolute value of the slope, $\text{Tan}\theta$ can be computed graphically from the profile chart.

4.2 Description of the Apparatus

Contact resistance data have been obtained from the apparatus in Figure 22. In a few words, the apparatus passes heat through two specimens in a vacuum environment. The three main sections of the apparatus are:

1. a vacuum chamber;
2. a refrigeration unit; and
3. a lever arrangement for applying an adjustable force to the test interface.

The vacuum system is basically a hollow aluminum cylinder which has been fabricated from four main sections. An upper cylinder is welded to a top plate. When the rig is in use, a removable lower cylinder with a flange seals up against an "O" ring and a bottom plate. The bottom plate is bolted to the supporting structure. The upper and lower cylinders are bolted together at their interface where another "O" ring allows for a vacuum seal. Connections with the vacuum pumps and the refrigeration unit are made through the bottom plate. Thermocouple wires, power lines

for the specimen heater, and a bellows for the loading mechanism enter through the top plate.

The vacuum is created by a forepump (Cenco HYVAC 14 rotary mechanical pump) and a 4-inch diameter diffusion pump (NRC model H4SP). A three-way valve allows the forepump to bring the system pressure down to 50 microns of mercury where activation of the diffusion pump will continue to lower the pressure to 15 microns of mercury.

The refrigeration unit, of course, supplies the low temperature sink for the heat fluxes that are passed through the test specimens. The unit is a 1-1/2 horsepower, Model 155 WFC, built by the Copeland Corporation. With its evaporator at 25 °F, it can receive up to 16,840 BTU/HR. Freon 12 serves as the refrigerant fluid. The magnitude of the heat-flux produced is crucial to contact resistance studies because with large loads too low a heat-flux will produce a negligible ΔT across the test interface.

A series of levers, supported by a welded steel frame, permits the application of force to the specimens at a ratio of 100 to 1. This dead-weight loading is transmitted into the vacuum system via a 15-convolution, 3-3/8-inch I.D. stainless steel bellows, manufactured by the Flexonics Division of the Universal Oil Products Company. At atmospheric pressure, the applied load can be adjusted between 0 and 20,000 pounds. When the system is evacuated, the minimum load is 163 pounds, due to the atmosphere pressing down on the 3-3/8-inch diameter bellows device.

In addition to the apparatus listed above, there is a water-flow cooler between the bellows and the heater. This cooler prevents the heater from raising the temperature of the rest of the chamber to a level

that would destroy the vacuum seals. The heater is powered by a 220 volt d.c. power source. A more detailed description of this apparatus may be found in Reference [12].

4.3 Experimental Procedure

Chromel-alumel thermocouples are covered with "Silver Goop" and inserted into the specimens. ("Silver Goop," manufactured by the Crawford Fitting Company, is a substance that provides a good thermal contact.) The thermocouple wires are then sealed in position with "White Epoxy," a product of the Hysol Division of the Dexter Corporation.

With the specimens inside, the vacuum chamber is sealed. The mechanical pump is switched on, and the system pressure is brought down to 50 microns of mercury. At this point the diffusion pump is activated to further lower the pressure to 15 microns of mercury. The applied load is now the minimum force of 163 pounds. After the water-flow cooler and the refrigeration unit are turned on, the heater is powered up to pass a heat-flux through the specimens.

Temperature readings are recorded from a thermocouple potentiometer every thirty minutes. When two successive readings are the same, it is assumed that steady state has been reached. The applied load is now increased, and the temperature-recording procedure is repeated. The applied load is always increased rather than decreased because the specimens may undergo a plastic (irreversible) deformation.

5. EXPERIMENTAL RESULTS AND DISCUSSION

The results of contact resistance experiments appear in Tables I and II and are plotted in Figures 23A and 23B. Also appearing are the predictions using Equation (2) for contact resistance with wavy surfaces, Equation (3) which includes the effects of both roughness and waviness, and Equation (5), an integral formula which assumes that the local interfacial flux is proportional to the local microscopic conductance and hence is a function of the local interfacial pressure. Equation (5) was solved on an I.B.M. 360 computer, using forty-four and eighty-nine radial increments (for the two different cases involved in the experiments) in a finite difference approximation of the integrals. The summation appearing in the macroscopic resistance term was evaluated using the first six terms of the series. The computer program for this equation appears in Appendix A. Equations (2) and (3) are given for the case of constant flux over the contour area, using two separate choices for the contour radius, a_w .

- a. $a_w = a_H$, the Hertzian (smooth surface) approximation; and
- b. $a_w = r_o$, the rough-surface contour radius determined from the pressure curves in Figures 7-16.

It has been stated earlier that Equation (5) is an upper bound for resistance (a lower bound for conductance). This indeed appears to be the case, as Equation (5) is the lowest curve in both Figures 23A and 23B. Using $a_w = a_H$, Equation (3) is very close to Equation (5). For the particular parameters involved in the experiments (for which the macroscopic conductance was the dominant factor), Equation (3) with $a_w = r_o$

gives the best prediction for the actual contact conductance (to within 25 per cent accuracy).

It is important to notice that in certain ranges of parameters, a wavy surface will yield a higher h if it is roughened. This is caused, as it is shown in this work, by an increase in the contour area. (The engagement of the two surfaces covers a larger area when roughness is present as in Figure 4B.) Experimentally, this was also observed by Clausing [1]. He, however, did not explain the phenomena.

Experiments performed in this work dealt with surfaces that were both rough and wavy. There was no need to experiment with rough, flat surfaces, because this topic has already been covered sufficiently, both experimentally and theoretically, in Reference [2], for example. Similarly, the case of smooth, wavy surfaces has been covered amply by authors such as Clausing [1].

6. CONCLUSIONS

From pressure distribution curves given in Figures 7-16, one can determine the actual contour area between two rough and wavy surfaces. In a certain range of parameters, this contour area is substantially larger than the value calculated from the Hertzian theory. Experiments were performed in this range, and three basic approaches for the calculation of contact conductance were applied to the results, including formulas based on

- a. the Hertzian contour area;
- b. the contour area predicted by this work; and
- c. an integral relation which uses the complete interfacial pressure distribution.

It is suggested that Equation (3) (which assumes constant flux over the the contour area) using contour radii predicted in this work is the best prediction for the cases involved in the experiments (in which the predominant resistance comes from macroscopic constriction). For those cases where microscopic resistance is primarily controlling the value of contact resistance, it is believed that the integral relation (Equation (5)) would yield the correct prediction. (For the case of a uniform pressure distribution between two flat, rough surfaces, Equation (5) reduces to one term, the microscopic constriction resistance.)

The main conclusion is that contact conductance can be increased for certain ranges of parameters by making surfaces rough. This thesis also identifies the range of parameters where roughness will substantially affect the interfacial pressure distribution between rough and wavy surfaces.

BIBLIOGRAPHY

1. Clausing, A. M. and Chao, B. T., "Thermal Contact Resistance in a Vacuum Environment," National Aeronautics and Space Administration, University of Illinois, ME-TN-242-1, August, 1965.
2. Cooper, M., Mikic, B. B., and Yovanovich, M. M., "Thermal Contact Conductance," International Journal of Heat and Mass Transfer, V. 12, 1969, pp. 279-300.
3. Greenwood, J. A., "Constriction Resistance and the Real Area in Contact," British Journal of Applied Physics, 17, 1966, pp. 1621-1632.
4. Greenwood, J. A., "The Area of Contact between a Rough Surface and a Plane," Burndy Research Report No. 25, Burndy Corporation, Norwalk, Connecticut, July 30, 1965.
5. Henry, J. J., "Thermal Resistance of Metals in Contact," M.I.T. S. M. Thesis, August, 1961.
6. Holm, R., Electric Contact Handbook, Springer Verlag, Berlin, 1958.
7. Kragelski, I. and Demkin, M., "Contact Area of Rough Surfaces," Wear, V. 3, 1966, pp. 170-187.
8. Mikic, B. B., "Thermal Constriction Resistance Due to Non-Uniform Surface Conditions; Contact Resistance at Non-Uniform Interface Pressure." (This article, written under contract with the National Aeronautics and Space Administration, has been accepted for publication in the International Journal of Heat and Mass Transfer.)
9. Mikic, B. B. and Flengas, S., "Thermal Contact Resistance in a Vacuum under Conditions of Non-Uniform Interface Pressure." M.I.T. Heat Transfer Laboratory Memorandum, 1967.

10. Mikic, B. B. and Rohsenow, W. M., "Thermal Contact Resistance," M.I.T. Report No. DSR 74542-41, September, 1966.
11. Timoshenko, S. and Goodier, J. N., Theory of Elasticity, New York, McGraw-Hill, 1951.
12. Velissaropoulos, P. D., "Apparatus for Measurement of Contact Resistance," M.I.T. S. M. Thesis, August, 1963.
13. Yovanovich, M. M., "Thermal Contact Conductance in a Vacuum," M.I.T. Report No. DSR 4542-39, November, 1965.
14. Yovanovich, M. M. and Rohsenow, W. M., "Influence of Surface Roughness upon Thermal Contact Resistance," M.I.T. Report No. 76361-48, June, 1967.

APPENDIX A

DERIVATION OF CONTACT RESISTANCE EQUATION

The equation developed by Mikic [8] for contact resistance (Equation 5) was derived as follows:

Figure 24A depicts a solid circular cylinder with a non-uniform heat transfer coefficient, h , on the $z = 0$ face. The sides are insulated, and heat-flow is assumed to be one-dimensional as $z \rightarrow \infty$. The flow of heat at the top surface is

$$Q = \int_A h (T_o - T_c) dA \quad (A1)$$

where T_o and T_c are defined in Figure 24A. The heat-flux over that surface is therefore

$$Q/A = T_o h_{av} - \frac{1}{A} \int_A T_c h dA \quad (A2)$$

where

$$h_{av} \equiv \frac{1}{A} \int_A h dA .$$

The total resistance from the surface to the ambient is

$$R \equiv \frac{T_o - T_s}{Q/A} \quad (A3)$$

where T_s is defined in Figure 24B.

To transform (A2) into the form of (A3), the term

$$\frac{1}{A} \int_A h T_s dA$$

can be subtracted from and added to the second and third terms of (A2), respectively to yield:

$$Q/A = (T_o - T_s) h_{av} - \frac{1}{A} \int (T_c - T_s) h dA . \quad (A4)$$

Thus we now have:

$$R = \frac{1}{h_{av}} + \frac{1}{Q} \int \frac{h}{A h_{av}} (T_c - T_s) dA . \quad (A5)$$

The second term on the right-hand side of (A5) is the constriction resistance:

$$R_c \equiv \frac{1}{Q} \int \frac{h}{h_{av}} (T_c - T_s) dA . \quad (A5.A)$$

This represents the difference in total resistance between the two cases pictured in Figure 25A.

Figure 25B illustrates the basic model for which Equation (5) was developed. At $z = 0$, h is a function of radius, and the sides are insulated. Also, $\frac{\partial T}{\partial z} = \text{constant}$ as $z \rightarrow \infty$.

The governing differential equation for the situation is

$$\nabla^2 T = 0 \quad (A6)$$

where ∇^2 is the Laplacian operator. For the given boundary conditions, the steady-state solution is

$$T_s = T_c - \frac{Q}{k\pi b^2} z + \sum_{n=1}^{\infty} C_n e^{-v_n z/b} J_0(v_n r/b) \quad (A7)$$

where v_n are the roots of

$$J_1(v_n) = 0 . \quad (A8)$$

Using relation (A8) and the approximation

$$\frac{[-k(\frac{\partial T}{\partial z})_{z=0}]_{\text{at } r}}{Q/A} \cong \frac{h(r)}{h_{av}} , \quad (A9)$$

Equation (A7) becomes

$$T_c - T_s = \frac{2Q}{\pi bk} \sum_{n=1}^{\infty} \frac{\int_0^1 \lambda J_0(v_n \lambda) f(\lambda) d\lambda}{v_n J_0^2(v_n)} J_0(v_n \lambda) \quad (A10)$$

where $\lambda \equiv r/b$ and $f(\lambda) \equiv h/h_{av}$. Combining (A5.A) and (A10) will yield

$$R_c = 4 \frac{b}{k} \sum_{n=1}^{\infty} \frac{[\int_0^1 \lambda f(\lambda) J_0(v_n \lambda) d\lambda]^2}{v_n J_0^2(v_n)} \quad (A11)$$

Contact conductance for purely rough surfaces with Gaussian surface height distributions has been shown in Reference [2] to be

$$h_c = 1.45 \frac{k \tan \theta}{\sigma} \left(\frac{P}{H}\right)^{0.985} \quad (A12)$$

where the variables have been defined in the nomenclature. By combining (A11) and (A12), Equation (A5) becomes Equation 5:

$$R = 0.345 \frac{\sigma}{k \tan \theta} \left[\int_0^1 \lambda \left(\frac{P}{H}\right)^{0.985} d\lambda\right]^{-1} + \frac{8b}{k} \sum_{n=1}^{\infty} \frac{[\int_0^1 \lambda (P/P_{av})^{0.985} J_0(v_n \lambda) d\lambda]^2}{v_n J_0^2(v_n)} \quad (5)$$

APPENDIX B
COMPUTER PROGRAMS

List of Fortran Variables Used in Programs

<u>Notation of This Thesis</u>	<u>Fortran Symbol</u>
a_H	AH
\bar{a}_H	AHB
b	B
\bar{F}	PLOAD, FBAR
H	H
$J_0(x)$	BESEL(X)
k	AK
p, or P	PRES, PRSS, PREZ, HRTZP (Hertzian) PRESH (Due to Hertzian Y)
\bar{p} , or \bar{P}	PBAR, PBAZ
Pl	PL
R	RES
R_i	RADI, RAD
R_1, R_2	R1, R2
r	R, RR, RHOM (radial position of dA)
$\bar{r}, d\bar{r}$	RB, DRB
$\bar{Y}(\bar{r})$	YB(I)
$\bar{Y}(0)$	YNB
$\lambda, d\lambda$	ALAM, DL
v_n where $J_1(v_n) = 0$	ANU(J)

Notation of This Thesis

Fortran Symbol

ρ $\bar{\rho}$

S

Tan θ

TAN

Tan₁ θ , Tan₂ θ

TAN1, TAN2

σ

SIGMA

σ_1, σ_2

SIGM1, SIGM2

PROGRAM TO DETERMINE DIMENSIONLESS PRESSURE
DISTRIBUTIONS BETWEEN ROUGH AND WAVY SURFACES

INPUT DATA	LINE NO.
a. MAX = Number of radial increments	31
b. $P\ell$, \bar{F}	33
c. YNB = first approximation for $\bar{Y}(0)$	38
OUTPUT DATA	
a. $P\ell$, \bar{F}	41
b. Dimensionless Hertzian pressures	57
c. Dimensionless Hertzian radius	68
d. First approximation for $\bar{Y}(\bar{r})$	69
e. First approximation for $\bar{P}(\bar{r})$	78
f. Second approximation for $\bar{P}(\bar{r})$	96
g. If any values of $\bar{Y}(\bar{r})$ are negative, they are written here.	151
h. Final values, $\bar{P}(\bar{r})$	229
i. Final values, $\bar{Y}(\bar{r})$	230
j. \bar{F} calculated from $\bar{P}(\bar{r})$	232
k. Dimensionless radial coordinates	235
l. $P\ell$, \bar{F}	239

```

DIMENSION PRSS(50),HRTZP(50),YB(50),PRESH(50),PBAR(50),Z(50),PBAZ(
150),W(50),PREZ(50),RTER(50),PRI(50)
C
C *****
C PROGRAM TO DETERMINE DIMENSIONLESS PRESSURE DISTRIBUTIONS BETWEEN
C ROUGH AND WAVY SURFACES
C *****
C
102 FORMAT(25X,F15.4)
103 FJRMAT(1H ,6E15.4)
105 FJRMAT(25X,15HHERTZIAN RADIUS)
107 FORMAT(1H ,40X,15HCALCULATED LOAD/)
108 FJRMAT(1H ,40X,E15.4)
109 FJRMAT(1H2,30X,27HFINAL PRESSURE DISTRIBUTION/)
112 FORMAT(E15.4)
114 FORMAT(1H ,30X,34HINTERMEDIATE PRESSURE DISTRIBUTION/)
117 FJRMAT(1H ,14HPLASTICITY(PL),6X,4HPBAR/)
118 FJRMAT(1H ,E15.4,5X,E15.4)
122 FJRMAT(2F10.3)
480 FJRMAT(1H ,22HPURE HERTZIAN PRESSURE/)
1001 FORMAT(I10)
1005 FJRMAT(1H ,8HYBAR(0)=,E15.4)
1008 FORMAT(1H ,8HYBAR(I)=/)
1011 FJRMAT(1H ,25HPBAR DUE TO HERTZIAN YBAR/)
4755 FORMAT(1H ,8HPBAZ(I)=/)
4756 FORMAT(1H ,30HPBAR(I)=(PBAR(I)+HRTZP(I))/2.0/)
A=0.0
COUNT=0.0
CHANGE=0.0
G=0.0
READ(5,1001) MAX
PI=3.14159
READ(5,122) PL,FBAR
AEAP=0.0
DO 8010 I=1,29
HRTZP(I)=0.0

```

```

PRES0001
PRES0002
PRES0003
PRES0004
PRES0005
PRES0006
PRES0007
PRES0008
PRES0009
PRES0010
PRES0011
PRES0012
PRES0013
PRES0014
PRES0015
PRES0016
PRES0017
PRES0018
PRES0019
PRES0020
PRES0021
PRES0022
PRES0023
PRES0024
PRES0025
PRES0026
PRES0027
PRES0028
PRES0029
PRES0030
PRES0031
PRES0032
PRES0033
PRES0034
PRES0035
PRES0036

```

8010	CONTINUE	PRES0037
	READ(5,112) YNB	PRES0038
8000	CONTINUE	PRFS0039
	WRITE(6,117)	PRES0040
	WRITE(6,118) PL,FBAR	PRES0041
	DO 75 I=1,MAX	PRFS0042
75	PRSS(I)=0.0	PRES0043
	PLDAD=FBAR	PRES0044
	RMAX=MAX-1	PRES0045
	MAXM1=MAX-1	PRFS0046
	AHB=1.333*((FBAR/PL)**.3333)	PRES0047
	AH=AHB	PRES0048
	AHSQ=AHB*AHB	PRES0049
	LL=(RMAX/4.0)+1.5	PRES0050
	DRB=(4.0*AHB)/RMAX	PRES0051
	DO 491 I=1,LL	PRES0052
	RB=FLOAT(I-1)*DRB	PRES0053
	HRTZP(I)=.477*(FBAR/AHSQ)*SQRT(1.0-(RB*RB/AHSQ))	PRES0054
491	CONTINUE	PRES0055
	WRITE(6,480)	PRES0056
	WRITE(6,103) (HRTZP(I),I=1,LL)	PRES0057
	DO 1 I=1,MAX	PRES0058
	RB=FLOAT(I-1)*DRB	PRES0059
	IF(RB-AHB)4,4,5	PRFS0060
4	YB(I)=0.0	PRES0061
	GO TO 1	PRES0062
5	SIDE=SQRT(RB*RB-AHSQ)	PRES0063
	Y3(I)=.5*(RB*RB-2.0*AHSQ*(1.0-.318*(((2.0-((RB/AH)**2.0))*ATAN(AH/	PRES0064
	1SIDE)+(((RB*RB)/(AHSQ))-1.0)**0.5))))	PRES0065
1	CONTINUE	PRES0066
	WRITE(6,105)	PRES0067
	WRITE(6,102) AHB	PRES0068
	WRITE(6,103) (YB(I),I=1,MAX)	PRES0069
	DO 200 I=1,MAX	PRES0070
	PRESH(I)=0.5*(1.0-ERF(YB(I)/(1.414))))	PRES0071
	PTEST=.001*PRESH(1)	PRES0072

```

IF(PRESH(I).LT.PTEST) GO TO 1984
200 CONTINUE
1984 MAX=I
    MAXM1=MAX-1
    WRITE(6,1011)
    WRITE(6,103) (PRESH(I),I=1,MAX)
    TEST1=.01*PRESH(1)
    AEAR=0.0
    DO 486 I=1,MAX
    RB=FLOAT(I-1)*DRB
486  AEAR=AEAR+PRESH(I)*RB*DRB
    FLOAD=2.0*PI*AEAR
    GO TO 195
1898 CONTINUE
    G=G+1.0
    IF(G.EQ.1.0) GO TO 8001
    GO TO 8003
8001 CONTINUE
    DO 8002 I=1,MAX
    PBAR(I)=(HRTZP(I)+PBAR(I))/2.0
    PR1(I)=PBAR(I)
8002 CONTINUE
    WRITE(6,4756)
    WRITE(6,103) (PBAR(I),I=1,MAX)
8003 CONTINUE
    DO 8004 I=1,MAX
    PBAR(I)=(PR1(I)+PBAR(I))/2.0
    PR1(I)=PBAR(I)
8004 CONTINUE
11  TEST1=.01*PBAR(1)
    COUNT=COUNT+1.0
    IF(COUNT-15.0)1972,1972,1979
1972 CONTINUE
    DO 85 I=1,MAX
85  PRSS(I)=PBAR(I)
    TEST=0.1*PBAR(1)

```

```

PRES0073
PRES0074
PRES0075
PRES0076
PRES0077
PRES0078
PRES0079
PRES0080
PRES0081
PRES0082
PRES0083
PRES0084
PRES0085
PRES0086
PRES0087
PRES0088
PRES0089
PRES0090
PRES0091
PRES0092
PRES0093
PRES0094
PRES0095
PRES0096
PRES0097
PRES0098
PRES0099
PRES0100
PRES0101
PRES0102
PRES0103
PRES0104
PRES0105
PRES0106
PRES0107
PRES0108

```

	N=MAX	PRES0109
	AREA=0.0	PRES0110
	DO 25 I=2,N	PRES0111
	RB=FLOAT(I-1)*DRB	PRES0112
	SUM=0.0	PRES0113
	ADD=2.0*SQR(T(PI)*DRB*PBAR(I)	PRES0114
	DO 26 K=1,N	PRES0115
	RHOM=FLOAT(K-1)*DRB	PRES0116
	SJM1=(2.0*RHOM*DRB*PBAR(K))/(RHOM*RHOM+RB*RB)**.5	PRES0117
	EP=2.0*RB*RHOM/(RB*RB+RHOM*RHOM)	PRES0118
	IF(EP-1.0)600,601,601	PRES0119
600	S3=0.0	PRES0120
	DO 300 J=1,5	PRES0121
	THETA=FLOAT(J-1)*PI/90.0+PI/180.0	PRES0122
	S=SQR(T(1.0-EP*CO(S(THETA))	PRES0123
	S3=S3+(PI/90.0)/S	PRES0124
300	CONTINUE	PRES0125
	S4=0.0	PRES0126
	DO 301 M=2,18	PRES0127
	THETA=FLOAT(M-1)*PI/18.0+PI/36.0	PRES0128
	S=SQR(T(1.0-EP*CO(S(THETA))	PRES0129
	S4=S4+(PI/18.0)/S	PRES0130
301	CONTINUE	PRES0131
	S1=S3+S4	PRES0132
	GO TO 602	PRES0133
601	S1=(2.0**0.5)*ALOG(8.0*RB/DRB)	PRES0134
602	SUM=SUM+(SUM1*S1)	PRES0135
26	CONTINUE	PRES0136
25	W(I)=(SUM+ADD)/PL	PRES0137
	W(1)=W(2)+(DRB*DRB)/2.0	PRES0138
	AEAP=0.0	PRES0139
	DO 50 I=1,MAX	PRES0140
	RB=FLOAT(I-1)*DRB	PRES0141
	RTER(I)=RB*RB/2.0	PRES0142
	YB(I)=RTER(I)-W(1)+W(I)+YNB	PRES0143
	PBAR(I)=0.5*(1.0-ERF(YB(I)/(2.0**0.5)))	PRES0144

50	CONTINUE	PRES0145
	DO 950 I=1,MAX	PRES0146
	IF(YB(I).LT.0.0) GO TO 8880	PRES0147
950	CONTINUE	PRES0148
	GO TO 1099	PRES0149
8880	CONTINUE	PRES0150
	WRITE(6,103) (YB(I),I=1,MAX)	PRES0151
482	CONTINUE	PRES0152
483	CONTINUE	PRES0153
	DO 484 I=1,MAX	PRES0154
	PBAR(I)=0.5*(1.0-ERF(YB(I)/(2.0**.5)))	PRES0155
484	CONTINUE	PRES0156
	GO TO 1099	PRES0157
195	CONTINUE	PRES0158
495	CONTINUE	PRES0159
	DO 295 I=1,MAX	PRES0160
	AEAP=0.0	PRES0161
295	YB(I)=YB(I)+YNB	PRES0162
	DO 99 I=1,MAX	PRES0163
	PBAR(I)=0.5*(1.0-ERF(YB(I)/(2.0**.5)))	PRES0164
99	CONTINUE	PRES0165
1099	CONTINUE	PRES0166
	DO 97 I=1,MAX	PRES0167
	IF(ABS(PRSS(I)-PBAR(I)).GT.TEST1) GO TO 75	PRES0168
97	CONTINUE	PRES0169
	AF=(FLOAD-PLOAD)/PLOAD	PRES0170
	IF(ABS(AF).GT.0.1) GO TO 76	PRES0171
	GO TO 16	PRES0172
76	CONTINUE	PRES0173
	DO 44 I=1,MAXM1	PRES0174
	RB=FLOAT(I-1)*DRB	PRES0175
44	AEAP=AEAP+PBAR(I)*RB*DRB	PRES0176
	FLOAD=2.0*PI*AEAP+(PBAR(1)*PI*DRB*DRB)/4.0	PRES0177
	AF=(FLOAD-PLOAD)/PLOAD	PRES0178
	AEAZ=0.0	PRES0179
	DO 196 I=1,MAX	PRES0180

	Z(I)=YB(I)-YB(1)	PRES0181
	PBAZ(I)=0.5*(1.0-ERF(Z(I)/(2.0**.5)))	PRES0182
196	CONTINUE	PRES0183
	DO 190 I=1,MAXM1	PRES0184
	RB=FLOAT(I-1)*DRB	PRES0185
190	AEAZ=AEA7+PBAZ(I)*RB*DRB	PRES0186
	FLJAZ=2.0*PI*AEAZ+(PBAZ(1)*PI*DRB*DRB)/4.0	PRES0187
	CHECK=FLJAZ-PLJAD	PRES0188
	DO 5000 I=1,MAX	PRES0189
5000	YB(I)=Z(I)	PRES0190
	IF(CHECK)9011,9011,192	PRES0191
9011	CONTINUE	PRES0192
	DO 9012 I=1,MAX	PRES0193
	PBAR(I)=PBAZ(I)	PRES0194
9012	CONTINUE	PRES0195
9013	CONTINUE	PRES0196
	GO TO 11	PRES0197
192	IF(PLJAD.GT.FLJAD) GO TO 193	PRES0198
	GO TO 191	PRES0199
193	AF=(FLJAD-PLJAD)/PLJAD	PRES0200
	IF(ABS(AF).LT.0.1) GO TO 1898	PRES0201
	IF(ABS(AF).LT.0.4) GO TO 476	PRES0202
	IF(ABS(AF).LT.0.6) GO TO 470	PRES0203
	IF(ABS(AF).LT.1.0) GO TO 477	PRES0204
	YNB=YNB*0.8	PRES0205
	GO TO 471	PRES0206
476	YNB=YNB*0.99	PRES0207
	GO TO 471	PRES0208
470	YNB=YNB*0.96	PRES0209
	GO TO 471	PRES0210
477	YNB=YNB*0.90	PRES0211
471	CONTINUE	PRES0212
	GO TO 195	PRES0213
191	AF=(FLJAD-PLJAD)/PLJAD	PRES0214
	IF(ABS(AF).LT.0.1) GO TO 1898	PRES0215
	IF(ABS(AF).LT.0.4) GO TO 478	PRES0216

```

IF (ABS(AF).LT.0.6) GO TO 473
IF (ABS(AF).LT.1.0) GO TO 479
YNB=YNB*1.2
GO TO 474
478 YNB=YNB*1.01
GO TO 474
473 YNB=YNB*1.04
GO TO 474
479 YNB=YNB*1.1
474 CONTINUE
GO TO 195
16 WRITE(6,109)
WRITE(6,103) (PBAR(I),I=1,MAX)
WRITE(6,103) (YB(I),I=1,MAX)
WRITE(6,107)
WRITE(6,108) FLOAD
DO 1970 I=1,MAX
RADIM=FLOAT(I-1)*DRB
WRITE(6,103) RADIM
1970 CONTINUE
1979 CONTINUE
WRITE(6,117)
WRITE(6,118) PL,FBAR
1973 CONTINUE
1978 CONTINUE
4901 CONTINUE
1971 CALL EXIT
END

```

```

PRES0217
PRES0218
PRES0219
PRES0220
PRES0221
PRES0222
PRES0223
PRES0224
PRES0225
PRES0226
PRES0227
PRES0228
PRES0229
PRES0230
PRES0231
PRES0232
PRES0233
PRES0234
PRES0235
PRES0236
PRES0237
PRES0238
PRES0239
PRES0240
PRES0241
PRES0242
PRES0243
PRES0244

```

USING EQUATION (5)

INPUT DATA	LINE NO.
a. $H, \sigma_1, \sigma_2, \tan_1 \theta, \tan_2 \theta$	34
b. k (thermal conductivity)	35
c. $R_1, R_2, \text{MAX} = \text{Number of pressures to be read}$	
$\text{in, } N = \text{number of roots of } J_1(v_n) = 0 \text{ to be read in}$	36
d. Dimensionless pressures	37
e. Roots of $J_1(v_n) = 0$	38
f. Dimensionless radial increment	39
g. Average pressure $\equiv F/A_{\text{app}}$	40
OUTPUT DATA	
a. INPUT DATA	93-100
b. Microscopic resistance term	102
c. Macroscopic resistance term	104
d. Total contact resistance	106

NOTE: The number appearing in the inequality in card 107 should be one less than the number of sets of input data.

	FUNCTION BESEL(X)	BESL0001
C		BESL0002
C	*****	BESL0003
C	BESSEL FUNCTION SJB-ROUTINE USED IN THE PROGRAM FOR CONTACT RESIS-	BESL0004
C	TANCE USING EQUATION (5)	BESL0005
C	*****	BESL0006
C		BESL0007
	IF(X-3.0)10,10,11	BESL0008
10	BESEL=1.0-2.24999*((X/3.0)**2.0)+1.26562*((X/3.0)**4.0)-.31638*((X	BESL0009
	1/3.0)**6.0)+.04444*((X/3.0)**8.0)-.00394*((X/3.0)**10.0)+.00021*((BESL0010
	1X/3.0)**12.0)	BESL0011
	RETURN	BESL0012
11	FZ=.79788-.00552*((3.0/X)**2.0)-.00009*((3.0/X)**3.0)+.00137*((3.0	BESL0013
	1/X)**4.0)-.00072*((3.0/X)**5.0)+.00014*((3.0/X)**6.0)	BESL0014
	THETA=X-.78539-.04166*(3.0/X)-.00004*((3.0/X)**2.0)+.00263*((3.0/X	BESL0015
	1)**3.0)-.00054*((3.0/X)**4.0)-.00029*((3.0/X)**5.0)+.00014*((3.0/X	BESL0016
	1)**6.0)	BESL0017
	BESEL=(FZ*COS(THETA))/(X**0.5)	BESL0018
	RETURN	BESL0019
	END	BESL0020

```

DIMENSION PAR(200),PRES(200),ANU(200)
RESI0001
RESI0002
RESI0003
RESI0004
RESI0005
RESI0006
RESI0007
RESI0008
RESI0009
RESI0010
RESI0011
RESI0012
RESI0013
RESI0014
RESI0015
RESI0016
RESI0017
RESI0018
RESI0019
RESI0020
RESI0021
RESI0022
RESI0023
RESI0024
RESI0025
RESI0026
RESI0027
RESI0028
RESI0029
RESI0030
RESI0031
RESI0032
RESI0033
RESI0034
RESI0035
RESI0036
100 FORMAT(5E15.4)
101 FORMAT(2E15.4,2I10)
103 FORMAT(6F10.4)
104 FORMAT(1H,6X,1HH,8X,5HSIGM1,10X,5HSIGM2/)
106 FORMAT(3F15.4)
107 FORMAT(1H,4HTAN1,10X,4HTAN2,11X,1HK/)
109 FORMAT(5X,3HMAX,5X,1HN,5X,2HR1,13X,2HR2/)
109 FORMAT(1H,17,16,2E15.4)
110 FORMAT(1H,23HDIMENSIONLESS PRESSURES/)
111 FORMAT(1H,18HCONTACT RESISTANCE/)
112 FORMAT(1H,E15.4,1X,16H(HR-F-F-T)/RTU/)
115 FORMAT(E15.4)
116 FORMAT(1H,4HDRB=E15.4)
117 FORMAT(1H,E15.4)
118 FORMAT(23HMAXP IS GREATER THAN LB/)
119 FORMAT(1X,10HSIGMA TERM/)
120 FORMAT(1X,6HB TERM/)
130 FORMAT(1X,17HAVERAGE PRESSURE=E15.4/)
131 FORMAT(E15.4)
132 FORMAT(1X,6HP/PAV=)
133 FORMAT(1H,5X,2HY=,9X,10HJ-ZERO(Y)=)
134 FORMAT(2E15.4)
135 FORMAT(F15.2)
R=0.5
BNUM=0.0
3333 CONTINUE
BNUM=BNUM+1.0
READ(5,100) H,SIGM1,SIGM2,TAN1,TAN2
READ(5,117) AK
READ(5,101) R1,R2,MAX,N

```

```

*****:*****:*****:*****:*****:*****:*****:*****:*****:*****:*****:*****:*****:*****:*****:*****
PROGRAM TO DETERMINE THERMAL CONTACT RESISTANCE USING EQUATION (5)
*****:*****:*****:*****:*****:*****:*****:*****:*****:*****:*****:*****:*****:*****:*****

```

```

READ(5,100) (PBAR(I),I=1,MAX)
READ(5,103) (ANU(J),J=1,N)
READ(5,115) DRB
READ(5,135) PAV
PTOT=0.0
TAN=(TAN1*TAN1+TAN2*TAN2)**0.5
SIGMA=(SIGM1*SIGM1+SIGM2*SIGM2)**0.5
RADI=(R1*R2)/(R1+R2)
DR=DRB*((RADI*SIGMA)**0.5)
MAXP=MAX+1
LB=B/DR
IF(LB-MAXP)51,51,49
49 CONTINUE
DJ 50 I=MAXP,LB
PBAR(I)=0.0
50 CONTINUE
GJ TJ 52
51 CONTINUE
WRITE(6,118)
52 CONTINUE
MAX=LB
PAVI=0.0
DO 2 K=1,MAX
RR=FLOAT(K-1)*DR
PRES(K)=H*PBAR(K)
PAVI=PAVI+PRES(K)*RR*DR
2 CONTINUE
WRITE(6,130) PAV
CK2=(0.345*SIGMA)/(AK*TAN)
CK3=(8.0*B)/AK
SUM=0.0
DO 3 I=1,MAX
R=FLOAT(I-1)*DR
ALAM=R/B
DL=DR/B
SUM=SUM+ALAM*(PBAR(I)**0.985)*DL

```

```

RESI0037
RESI0038
RESI0039
RESI0040
RESI0041
RESI0042
RESI0043
RESI0044
RESI0045
RESI0046
RESI0047
RFSI0048
RESI0049
RESI0050
RESI0051
RESI0052
RESI0053
RESI0054
RESI0055
RESI0056
RESI0057
RESI0058
RESI0059
RESI0060
RESI0061
RESI0062
RESI0063
RESI0064
RESI0065
RESI0066
RESI0067
RFSI0068
RESI0069
RESI0070
RESI0071
RFSI0072

```

3	CONTINUE	RESI0073
	TERM1=CK2/SUM	RESI0074
	SUMMA=0.0	RESI0075
	DO 5 J=1,N	RESI0076
	X=ANU(J)	RESI0077
	SUM1=0.0	RESI0078
	DO 4 I=1,MAX	RESI0079
	R=FLJAT(I-1)*DR	RESI0080
	ALAM=R/B	RESI0081
	Y=ANJ(J)*ALAM	RESI0082
	SUM1=SUM1+ALAM*((PRES(I)/PAV)**0.985)*(BESEL(Y))*JL	RESI0083
4	CONTINUE	RESI0084
	SUMMA=SUMMA+(SUM1*SUM1)/(ANU(J)*(ABS(BESEL(X))**2.0))	RESI0085
	WRITE(6,131) SUM1	RESI0086
5	CONTINUE	RESI0087
	TERM2=CK3*SUMMA	RESI0088
	RES=(TERM1+TERM2)/12.0	RESI0089
	ANS1=TERM1/12.0	RESI0090
	ANS2=TERM2/12.0	RESI0091
	WRITE(6,104)	RESI0092
	WRITE(6,106) H,SIGM1,SIGM2	RESI0093
	WRITE(6,116) DRB	RESI0094
	WRITE(6,107)	RESI0095
	WRITE(6,106) TAN1,TAN2,AK	RESI0096
	WRITE(6,108)	RESI0097
	WRITE(6,109) MAX,N,R1,R2	RESI0098
	WRITE(6,110)	RESI0099
	WRITE(6,100) (PRAR(I),I=1,MAX)	RESI0100
	WRITE(6,119)	RESI0101
	WRITE(6,112) ANS1	RESI0102
	WRITE(6,120)	RESI0103
	WRITE(6,112) ANS2	RESI0104
	WRITE(6,111)	RESI0105
	WRITE(6,112) RES	RESI0106
	IF(BNUM.GT.6.0) GO TO 3334	RESI0107
	GO TO 3333	RESI0108

3334 CONTINUE
C K IS IN (BTU/HR-F-FT)
C SIGMA AND B ARE IN INCHES
C RESISTANCE IS IN (HR-F-FT-FT)/BTU
CALL EXIT
END

RESI0109
RESI0110
RESI0111
RESI0112
RESI0113
RESI0114

APPENDIX C

TABLES OF COORDINATES FOR PRESSURE DISTRIBUTIONS

$$P_1 = .002$$

$$\bar{F} = .005$$

\bar{r}	\bar{P}
0.000	.00066
0.302	.00066
0.603	.00061
0.905	.00054
1.206	.00046
1.508	.00034
1.809	.00019
2.111	.00007
2.412	.00000

P1 = .004

$\bar{F} = .005$		$\bar{F} = .010$	
\bar{r}	\bar{P}	\bar{r}	\bar{P}
0.000	.00097	0.000	.00132
0.239	.00097	0.302	.00132
0.478	.00089	0.603	.00121
0.718	.00081	0.905	.00109
0.957	.00068	1.206	.00092
1.197	.00052	1.508	.00069
1.436	.00034	1.809	.00040
1.675	.00016	2.111	.00014
1.915	.00005	2.412	.00002
2.154	.00001	2.714	.00000
2.393	.00000		

P1 = .006

$\bar{F} = .010$

$\bar{F} = .015$

\bar{r}	\bar{P}	\bar{r}	\bar{P}
0.000	.00164	0.000	.00199
0.263	.00164	0.302	.00199
0.527	.00152	0.603	.00183
0.790	.00136	0.905	.00165
1.054	.00115	1.206	.00139
1.317	.00087	1.508	.00103
1.580	.00054	1.809	.00062
1.844	.00024	2.111	.00023
2.107	.00006	2.412	.00004
2.371	.00000	2.714	.00000

P1 = .01

\bar{F} = .02

\bar{r}	\bar{P}
0.000	.00293
0.279	.00293
0.559	.00270
0.839	.00243
1.120	.00204
1.400	.00153
1.679	.00093
1.959	.00039
2.239	.00009
2.519	.00000

P1 = .02

$\bar{F} = .040$

$\bar{F} = .060$

\bar{r}	\bar{P}	\bar{r}	\bar{P}
0.000	.00590	0.000	.00685
0.279	.00590	0.320	.00685
0.559	.00545	0.641	.00631
0.839	.00492	0.961	.00568
1.120	.00416	1.282	.00476
1.400	.00316	1.602	.00350
1.679	.00199	1.922	.00198
1.959	.00089	2.243	.00068
2.239	.00023	2.563	.00010
2.519	.00003	2.884	.00000
2.799	.00000		

$\bar{F} = .080$

\bar{r}	\bar{P}
0.000	.00765
0.353	.00765
0.705	.00701
1.058	.00629
1.411	.00528
1.763	.00384
2.116	.00203
2.469	.00054
2.821	.00005

P1 = .04

$\bar{F} = .13$		$\bar{F} = .16$	
\bar{r}	\bar{P}	\bar{r}	\bar{P}
0.000	.01412	0.000	.01556
0.320	.01412	0.353	.01556
0.641	.01305	0.705	.01433
0.961	.01182	1.058	.01294
1.282	.01004	1.411	.01090
1.602	.00763	1.763	.00807
1.922	.00469	2.116	.00458
2.243	.00189	2.469	.00145
2.563	.00036	2.821	.00016
2.884	.00002	3.174	.00000
3.204	.00000		

$$P1 = .05$$

$$\bar{F} = .2$$

\bar{r}	\bar{P}
0.000	.01861
0.353	.01861
0.705	.01708
1.058	.01530
1.411	.01273
1.763	.00916
2.116	.00487
2.469	.00140
2.821	.00014
3.174	.00000
3.527	.00000

P1 = .1

$\bar{F} = .25$

$\bar{F} = .5$

\bar{r}	\bar{P}	\bar{r}	\bar{P}
0.000	.03056	0.000	.04072
0.302	.03056	0.367	.04072
0.603	.02825	0.734	.03758
0.905	.02540	1.100	.03397
1.206	.02138	1.467	.02878
1.508	.01609	1.834	.02169
1.809	.00992	2.201	.01282
2.111	.00429	2.567	.00439
2.412	.00104	2.934	.00053
2.714	.00011	3.301	.00002
3.015	.00000	3.668	.00000

$\bar{F} = .6$

\bar{r}	\bar{P}
0.000	.04503
0.415	.04503
0.829	.04122
1.244	.03693
1.658	.03079
2.073	.02210
2.488	.01103
2.902	.00232
3.317	.00009
3.731	.00000

P1 = .20

$\bar{F} = .2$		$\bar{F} = .4$	
\bar{r}	\bar{P}	\bar{r}	\bar{P}
0.000	.03741	0.000	.05564
0.222	.03741	0.280	.05564
0.444	.03543	0.560	.05174
0.667	.03010	0.840	.04685
0.889	.02685	1.120	.04008
1.111	.02071	1.400	.03131
1.333	.01446	1.679	.02105
1.555	.00859	1.959	.01096
1.777	.00409	2.239	.00378
1.999	.00145	2.519	.00073
2.222	.00036	2.799	.00007
2.444	.00006	3.079	.00000
2.666	.00000		

$\bar{F} = .6$		$\bar{F} = .8$	
\bar{r}	\bar{P}	\bar{r}	\bar{P}
0.000	.06558	0.000	.07312
0.320	.06558	0.353	.07312
0.641	.06071	0.705	.06748
0.961	.05472	1.058	.06068
1.282	.04625	1.411	.05091
1.602	.03506	1.763	.03767
1.922	.02189	2.116	.02191
2.243	.00954	2.469	.00788
2.563	.00223	2.821	.00119
2.884	.00021	3.174	.00005
3.204	.00000	3.527	.00000

P1 = .20

$\bar{F} = 1$		$\bar{F} = 1.3$	
\bar{r}	\bar{P}	\bar{r}	\bar{P}
0.000	.08200	0.000	.09035
0.379	.08200	0.404	.09035
0.759	.07567	0.807	.08344
1.114	.06825	1.211	.07551
1.520	.05759	1.615	.06403
1.899	.04296	2.018	.04827
2.279	.02486	2.422	.02826
2.659	.00818	2.826	.00897
3.039	.00090	3.229	.00079
3.419	.00002	3.633	.00001
3.799	.00000	4.037	.00000

$\bar{F} = 1.4$		$\bar{F} = 1.6$	
\bar{r}	\bar{P}	\bar{r}	\bar{P}
0.000	.09551	0.000	.09919
0.425	.09551	0.444	.09919
0.850	.08810	0.889	.09136
1.275	.08002	1.333	.08232
1.700	.06825	1.777	.06892
2.125	.05113	2.222	.05033
2.550	.02863	2.666	.02679
2.975	.00791	3.110	.00611
3.400	.00049	3.554	.00023
3.825	.00000	3.999	.00000

$$P1 = .20$$

$$\bar{F} = 1.7$$

\bar{r}	\bar{P}
0.000	.10280
0.462	.10280
0.924	.09467
1.386	.08538
1.848	.07131
2.310	.05126
2.773	.02578
3.235	.00489
3.697	.00011
4.159	.00000

P1 = .30

$\bar{F} = .2$		$\bar{F} = .4$	
\bar{r}	\bar{P}	\bar{r}	\bar{P}
0.000	.04341	0.000	.06279
0.194	.04341	0.245	.06279
0.388	.04109	0.489	.05844
0.582	.03840	0.734	.05259
0.776	.03203	0.978	.04461
0.970	.02575	1.223	.03477
1.164	.01922	1.467	.02403
1.359	.01283	1.712	.01364
1.553	.00742	1.956	.00588
1.747	.00357	2.201	.00174
1.941	.00137	2.445	.00032
		2.690	.00003
		2.934	.00000

$\bar{F} = .6$		$\bar{F} = .8$	
\bar{r}	\bar{P}	\bar{r}	\bar{P}
0.000	.07933	0.000	.10440
0.280	.07933	0.308	.10440
0.559	.07374	0.616	.10020
0.837	.06653	0.924	.08434
1.120	.05658	1.232	.06819
1.400	.04384	1.540	.05281
1.679	.02921	1.848	.03449
1.959	.01511	2.157	.01671
2.239	.00525	2.465	.00484
2.519	.00103	2.773	.00066
2.799	.00099	3.081	.00003
3.079	.00000	3.389	.00000

P1 = .30

$\bar{F} = 1.2$

$\bar{F} = 1.5$

\bar{r}	\bar{P}	\bar{r}	\bar{P}
0.000	.11040	0.000	.11940
0.353	.11040	0.379	.11940
0.705	.10230	0.759	.11030
1.058	.09235	1.140	.09936
1.411	.07819	1.520	.08357
1.763	.05913	1.899	.06189
2.116	.03619	2.279	.03556
2.469	.01456	2.659	.01198
2.821	.00268	3.039	.00144
3.174	.00015	3.419	.00004
3.527	.00000	3.799	.00000

$\bar{F} = 2$

$\bar{F} = 2.6$

\bar{r}	\bar{P}	\bar{r}	\bar{P}
0.000	.13300	0.000	.15240
0.418	.13300	0.450	.15240
0.836	.12230	0.901	.14070
1.254	.11000	1.351	.12800
1.672	.09227	1.802	.10950
2.091	.06731	2.252	.08245
2.509	.03580	2.702	.04636
2.927	.00912	3.153	.01238
3.345	.00054	3.603	.00060
3.736	.00000	4.054	.00000

P1 = .30

$\bar{F} = 3.1$		$\bar{F} = 3.4$	
\bar{r}	\bar{P}	\bar{r}	\bar{P}
0.000	.19610	0.000	.16930
0.479	.19610	0.499	.16930
0.957	.18000	0.998	.15550
1.436	.15500	1.497	.14050
1.914	.12160	1.996	.11900
2.393	.08924	2.495	.08791
2.872	.04903	2.994	.04557
3.350	.01158	3.493	.00824
3.829	.00035	3.992	.00012
4.307	.00000	4.491	.00000

P1 = .40

$\bar{F} = .1$		$\bar{F} = .2$	
\bar{r}	\bar{P}	\bar{r}	\bar{P}
0.000	.02907	0.000	.04654
0.140	.02907	0.176	.04654
0.279	.02770	0.353	.04411
0.419	.02567	0.529	.04010
0.559	.02301	0.705	.03503
0.699	.01985	0.882	.02884
0.839	.01638	1.058	.02233
0.979	.01281	1.234	.01584
1.120	.00941	1.411	.01008
1.260	.00644	1.587	.00561
1.400	.00405	1.763	.00265
1.540	.00231	1.940	.00103
1.680	.00118	2.116	.00032
1.820	.00054	2.292	.00008
1.959	.00021	2.469	.00001
2.099	.00007	2.645	.00000
2.239	.00002		
2.379	.00000		

P1 = .40

$\bar{F} = .3$		$\bar{F} = .4$	
\bar{r}	\bar{P}	\bar{r}	\bar{P}
0.000	.05887	0.000	.07284
0.202	.05887	0.222	.07284
0.404	.05519	0.444	.06905
0.606	.05004	0.667	.04606
0.807	.04320	0.889	.05324
1.009	.03497	1.111	.04192
1.211	.02603	1.333	.03019
1.413	.01720	1.555	.01883
1.615	.00972	1.777	.00963
1.817	.00450	1.999	.00378
2.019	.00162	2.222	.00106
2.220	.00044	2.444	.00020
2.422	.00008	2.666	.00002
2.624	.00001	2.888	.00000
2.826	.00000		

P1 = .40

$\bar{F} = .5$

$\bar{F} = 1.0$

\bar{r}	\bar{P}	\bar{r}	\bar{P}
0.000	.07819	0.000	.14330
0.239	.07819	0.302	.14330
0.479	.07288	0.603	.13600
0.718	.06563	0.905	.12600
0.957	.05584	1.206	.09847
1.197	.04382	1.508	.07404
1.436	.03064	1.809	.04977
1.675	.01795	2.111	.02613
1.915	.00819	2.412	.00886
2.154	.00267	2.714	.00154
2.393	.00057	3.015	.00011
2.633	.00007	3.317	.00000
2.872	.00000		

$\bar{F} = 1.6$

$\bar{F} = 2.0$

\bar{r}	\bar{P}	\bar{r}	\bar{P}
0.000	.16620	0.000	.16250
0.345	.16620	0.380	.16250
0.690	.15000	0.760	.15070
1.035	.13430	1.140	.13660
1.381	.10980	1.520	.11630
1.726	.08462	1.899	.08867
2.071	.05520	2.279	.05445
2.416	.02549	2.659	.02113
2.761	.00606	3.039	.00327
3.106	.00051	3.419	.00012
3.451	.00001	3.799	.00000
3.797	.00000		

P1 = .40

$\bar{F} = 2.3$

$\bar{F} = 3$

\bar{r}	\bar{P}	\bar{r}	\bar{P}
0.000	.16910	0.000	.18660
0.409	.16910	0.434	.18660
0.818	.15580	0.869	.17200
1.228	.13980	1.305	.15490
1.637	.11670	1.739	.13030
2.046	.08486	2.174	.09618
2.455	.04595	2.609	.05282
2.864	.01283	3.044	.01389
3.274	.00097	3.479	.00077
3.683	.00001	3.914	.00000
4.092	.00000		

$\bar{F} = 3.5$

$\bar{F} = 4.0$

\bar{r}	\bar{P}	\bar{r}	\bar{P}
0.000	.20270	0.000	.21280
0.462	.20270	0.487	.21280
0.924	.18720	0.973	.19570
1.386	.16970	1.459	.17680
1.848	.14390	1.946	.14950
2.310	.10610	2.432	.10930
2.773	.05679	2.919	.05533
3.235	.01355	3.405	.01040
3.697	.00051	3.892	.00020
4.159	.00000	4.378	.00000

P1 = .50

$\bar{F} = 0.1$		$\bar{F} = 0.2$	
\bar{r}	\bar{P}	\bar{r}	\bar{P}
0.000	.03035	0.000	.04989
0.130	.03035	0.164	.04989
0.260	.02906	0.327	.04730
0.390	.02716	0.491	.04357
0.520	.02259	0.654	.03869
0.650	.02155	0.819	.02909
0.780	.01712	0.982	.02375
0.910	.01395	1.146	.01934
1.039	.01119	1.310	.01312
1.169	.00808	1.473	.00802
1.299	.00546	1.637	.00432
1.429	.00342	1.801	.00201
1.559	.00197	1.964	.00079
1.689	.00103	2.128	.00025
1.819	.00049	2.292	.00007
1.949	.00020	2.455	.00001
2.079	.00008	2.619	.00000
2.209	.00002		
2.339	.00000		

P1 = .50

$\bar{F} = 0.3$		$\bar{F} = 0.4$	
\bar{r}	\bar{p}	\bar{r}	\bar{p}
0.000	.06450	0.000	.07678
0.187	.06450	0.206	.07678
0.375	.06118	0.413	.07269
0.562	.05880	0.619	.06960
0.750	.04869	0.825	.05661
0.937	.03417	1.031	.04537
1.124	.03037	1.237	.03365
1.312	.02100	1.444	.02217
1.499	.01288	1.650	.01248
1.686	.00677	1.856	.00572
1.874	.00294	2.062	.00203
2.061	.00102	2.269	.00053
2.249	.00027	2.475	.00009
2.436	.00005	2.681	.00001
2.623	.00000	2.887	.00000

P1 = .50

$\bar{F} = 0.5$		$\bar{F} = 1$	
\bar{r}	\bar{P}	\bar{r}	\bar{P}
0.000	.08860	0.000	.12320
0.222	.08860	0.279	.12320
0.444	.08396	0.559	.11450
0.666	.07700	0.839	.10280
0.889	.06489	1.112	.08680
1.111	.05131	1.400	.06657
1.333	.03720	1.679	.04418
1.555	.02347	1.959	.02282
1.777	.01222	2.239	.00806
1.999	.00492	2.519	.00165
2.222	.00143	2.799	.00017
2.444	.00028	3.079	.00000
2.666	.00003		
2.888	.00000		

P1 = .50

$\bar{F} = 1.6$

$\bar{F} = 2$

\bar{r}	\bar{P}	\bar{r}	\bar{P}
0.000	.16010	0.000	.18160
0.320	.16010	0.353	.18160
0.641	.14910	0.705	.16870
0.961	.13520	1.058	.15280
1.282	.11580	1.411	.13030
1.602	.09038	1.763	.10030
1.922	.05998	2.116	.06408
2.243	.02954	2.469	.02833
2.563	.00861	2.821	.00624
2.884	.00112	3.174	.00045
3.204	.00005	3.527	.00000
3.524	.00000		

$\bar{F} = 3$

$\bar{F} = 4$

\bar{r}	\bar{P}	\bar{r}	\bar{P}
0.000	.21710	0.000	.23810
0.404	.21710	0.443	.23810
0.807	.20130	0.889	.21990
0.211	.18240	1.333	.19850
1.615	.15520	1.777	.16740
2.018	.11810	2.222	.12400
2.422	.07195	2.666	.06894
2.826	.02652	3.110	.01859
3.229	.00334	3.554	.00101
3.633	.00007	3.999	.00000
4.037	.00000		

P1 = .50

$\bar{F} = 5.3$

$\bar{F} = 5.5$

\bar{r}	\bar{P}	\bar{r}	\bar{P}
0.000	.26970	0.000	.27400
0.497	.26970	0.485	.27400
0.994	.24820	0.969	.25380
1.491	.22350	1.455	.23050
1.988	.18800	1.940	.19600
2.485	.13720	2.425	.14760
2.982	.06998	2.909	.08466
3.479	.01309	3.394	.02249
3.976	.00023	3.879	.00083
4.473	.00000	4.364	.00000

P1 = .60

$\bar{F} = .5$

$\bar{F} = .9$

\bar{r}	\bar{P}	\bar{r}	\bar{P}
0.000	.09278	0.000	.13250
0.209	.09278	0.263	.13250
0.418	.08787	0.526	.12340
0.627	.08000	0.790	.11120
0.836	.06858	1.054	.09446
1.045	.05507	1.317	.07363
1.254	.04093	1.580	.05048
1.463	.02701	1.844	.02816
1.673	.01521	2.107	.01155
1.882	.00694	2.371	.00307
2.091	.00244	2.634	.00047
2.300	.00062	2.897	.00004
2.509	.00011	3.161	.00000
2.718	.00001		
2.927	.00000		

$\bar{F} = 1.4$

$\bar{F} = 2.2$

\bar{r}	\bar{P}	\bar{r}	\bar{P}
0.000	.16470	0.000	.24200
0.302	.16470	0.332	.24200
0.603	.15310	0.664	.23800
0.905	.13790	0.996	.20000
1.206	.11660	1.327	.16730
1.508	.08929	1.659	.12580
1.809	.05843	1.991	.08412
2.111	.02877	2.323	.04265
2.412	.00900	2.655	.01276
2.714	.00144	2.987	.00162
3.015	.00009	3.319	.00006
3.317	.00000	3.650	.00000

P1 = .60

$\bar{F} = 3$		$\bar{F} = 4$	
\bar{r}	\bar{P}	\bar{r}	\bar{P}
0.000	.23870	0.000	.27230
0.379	.23870	0.418	.27230
0.759	.22160	0.836	.25280
1.140	.20090	1.254	.22970
1.520	.17150	1.672	.19650
1.899	.13200	2.091	.15090
2.279	.08380	2.509	.09325
2.659	.03514	2.927	.03470
3.039	.00631	3.345	.00414
3.419	.00028	3.763	.00007
3.799	.00000	4.181	.00000

$\bar{F} = 5$		$\bar{F} = 6$	
\bar{r}	\bar{P}	\bar{r}	\bar{P}
0.000	.28120	0.000	.37270
0.450	.28120	0.479	.37270
0.901	.25950	0.957	.35000
1.351	.23340	1.436	.29740
1.802	.19570	1.914	.23730
2.252	.14280	2.393	.17740
2.702	.07633	2.872	.10300
3.153	.01889	3.350	.02892
3.603	.00087	3.829	.00129
4.054	.00000	4.307	.00000

TABLE I

EXPERIMENTAL DATA

Stainless Steel (303)

Specimen Pair No. 1

$k = 10.0 \text{ BTU/HR.FT.}^{\circ}\text{F}$

<u>Specimen 1.1</u>	<u>Specimen 1.2</u>	<u>Combined Values</u>
$\sigma_1 = 81 \mu''$	$\sigma_2 = 69 \mu''$	$\sigma = 106 \mu''$
$R_1 = 10.4''$	$R_2 = 8.4''$	$R_1 = 4.65''$
$\text{Tan}_1\theta = .0512$	$\text{Tan}_2\theta = .0378$	$\text{Tan}\theta = .0635$

<u>F(Applied Load in Lbs.)</u>	<u>h(BTU/HR.FT²°F)</u>
165	10.7
265	12.5
365	13.9
765	20.0
1165	26.0
2165	32.8
3165	41.0
5165	54.7
7165	62.5
9765	85.7

TABLE II
EXPERIMENTAL DATA

Stainless Steel (303)

Specimen Pair No. 2

$k = 10.0 \text{ BTU/HR.FT}^{\circ}\text{F}$

<u>Specimen 2.1</u>	<u>Specimen 2.2</u>	<u>Combined Values</u>
$\sigma_1 = 69 \mu''$	$\sigma_2 = 0 \mu''$	$\sigma = 69 \mu''$
$R_1 = 250''$	$R_2 = 156''$	$R_1 = 96''$
$\text{Tan}_1\theta = .068$	$\text{Tan}_2\theta = 0$	$\text{Tan}\theta = .068$

<u>F(Lbs.)</u>	<u>h(BTU/HR.FT²°F)</u>
165	49
265	71
365	88
565	101
765	124
1165	208

FIGURES

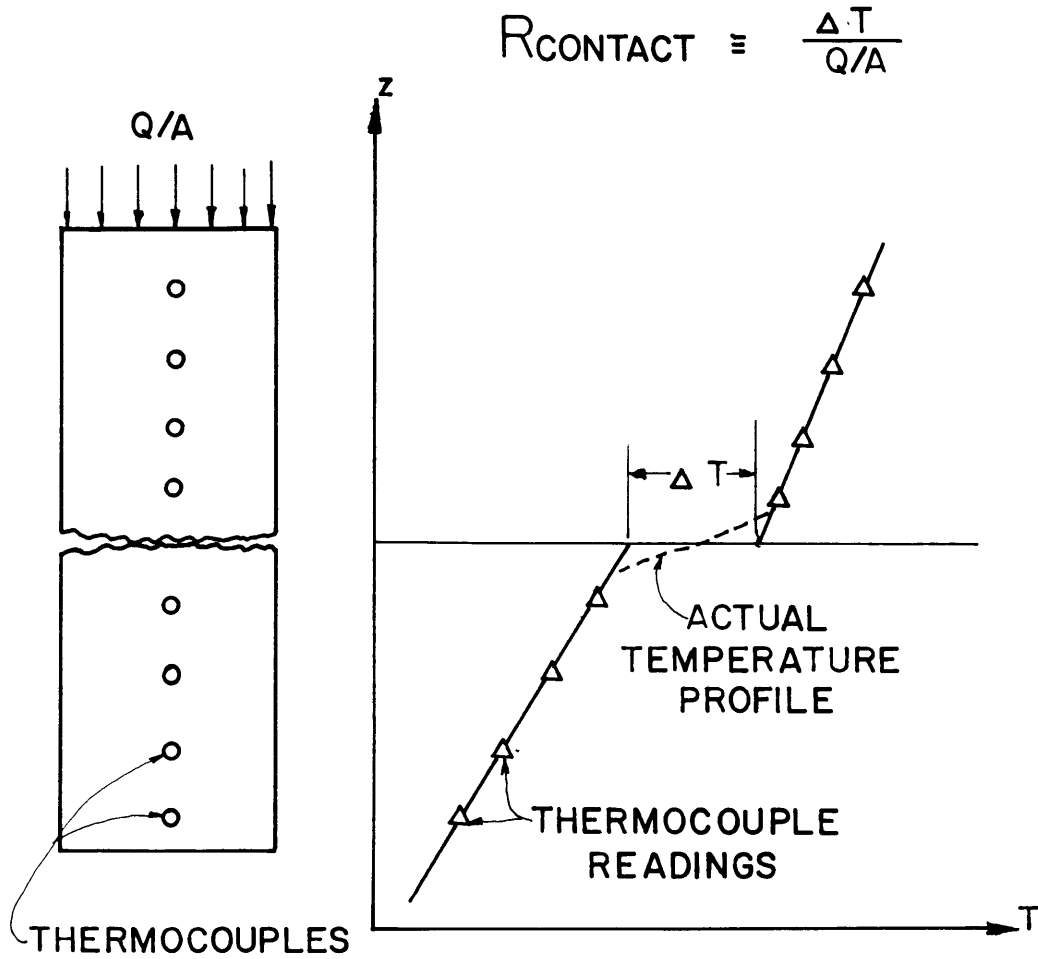


FIG. 1 DEFINITION OF CONTACT RESISTANCE

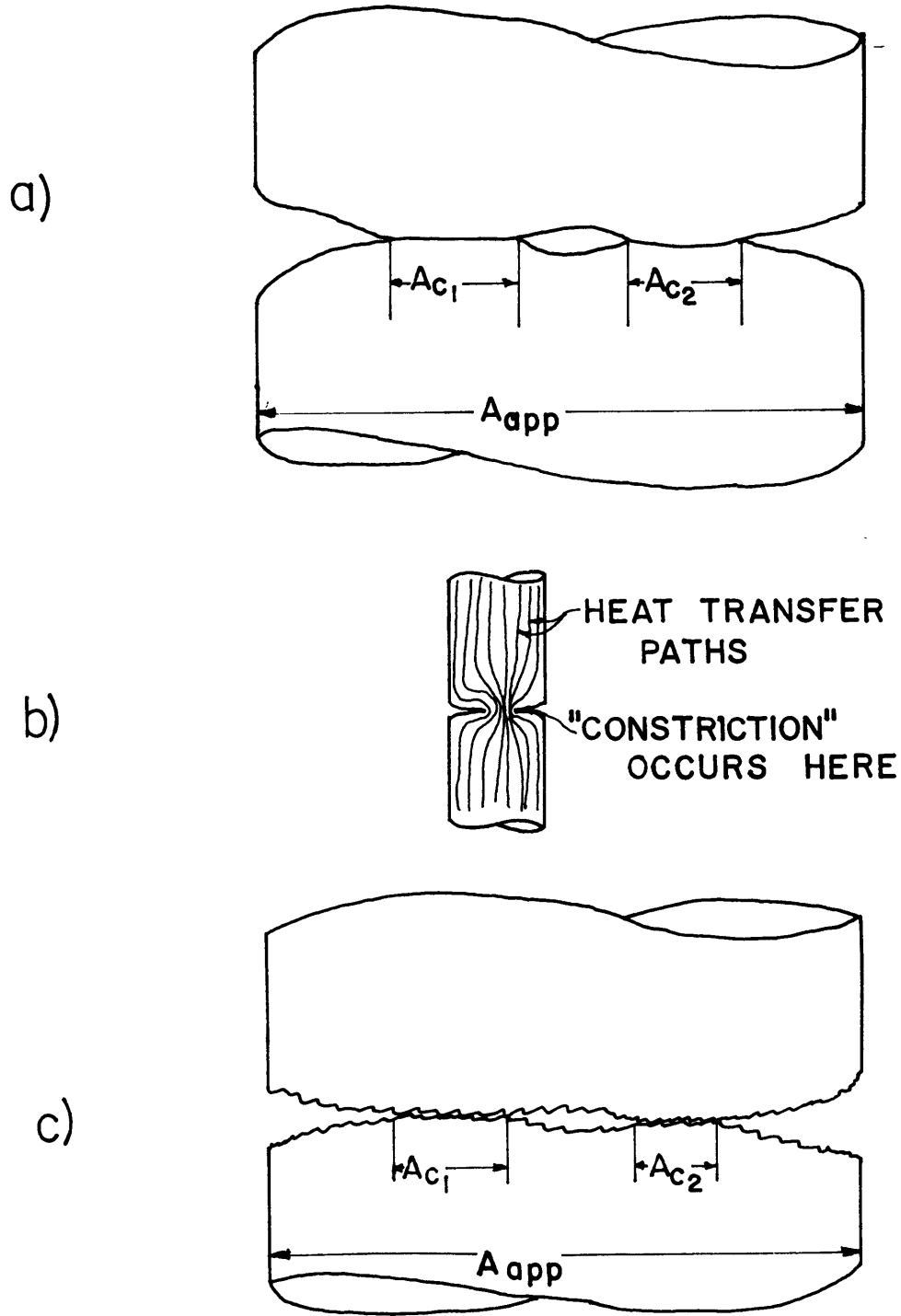


FIG. 2 SURFACE CONTACTS

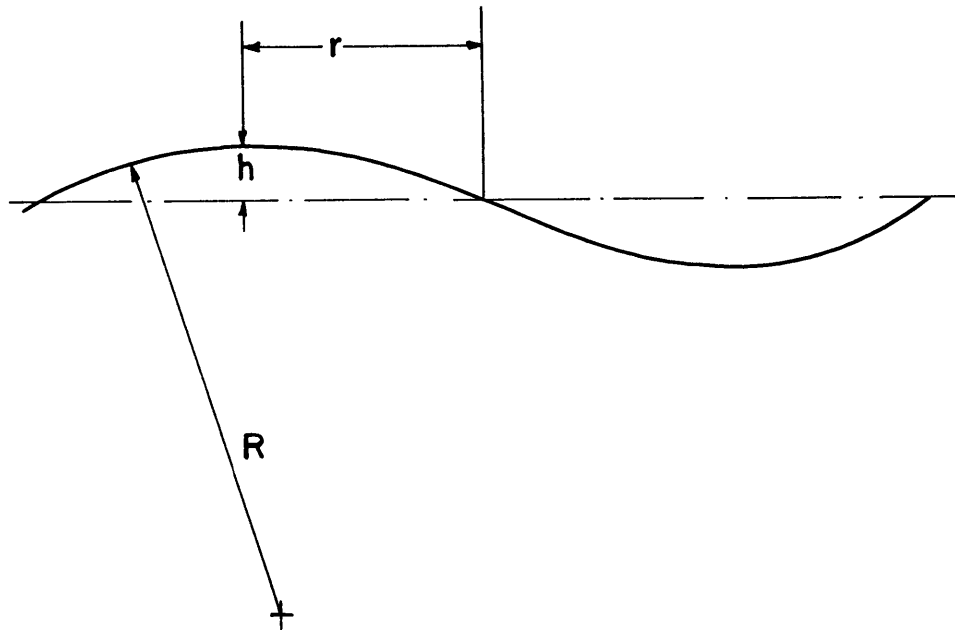


FIG. 3 SURFACE WAVINESS

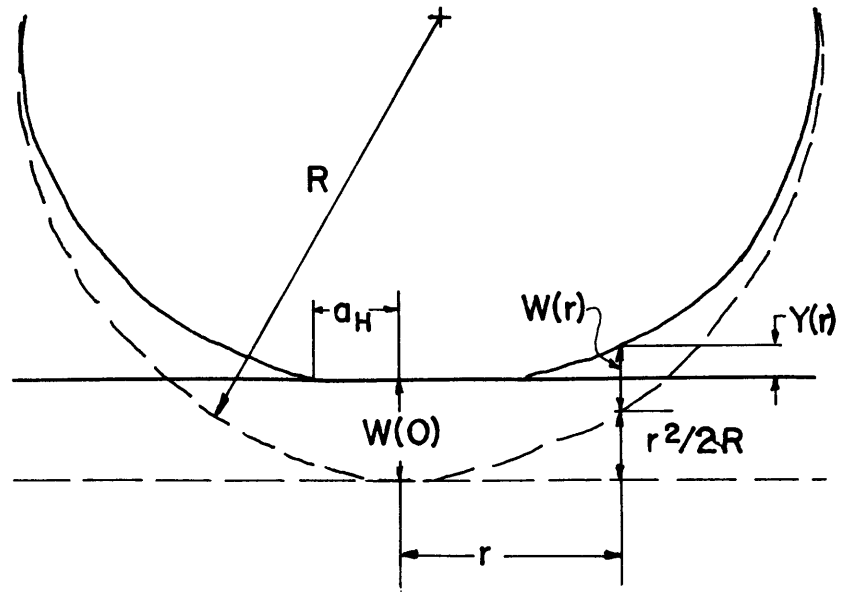


FIG. 4a SMOOTH SPHERE PRESSED AGAINST RIGID PLANE

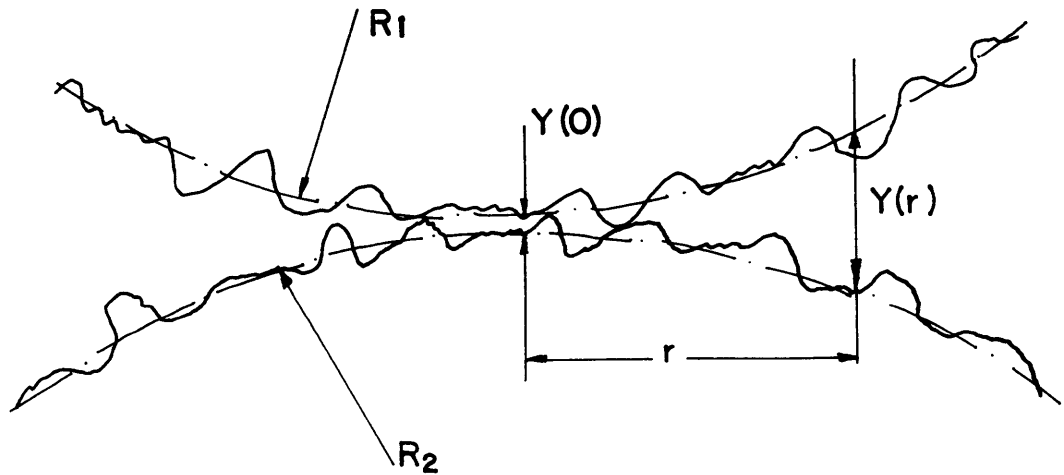


FIG. 4b TWO ROUGH SURFACES PRESSED TOGETHER

$$w(r) = \frac{1-\nu^2}{\pi E} \iint \frac{p}{r} dA$$

POINT (A) IS A POINT WHERE $w(r)$ IS TO BE COMPUTED

POINT (B) IS THE ORIGIN OF A CIRCULAR COORDINATE SYSTEM

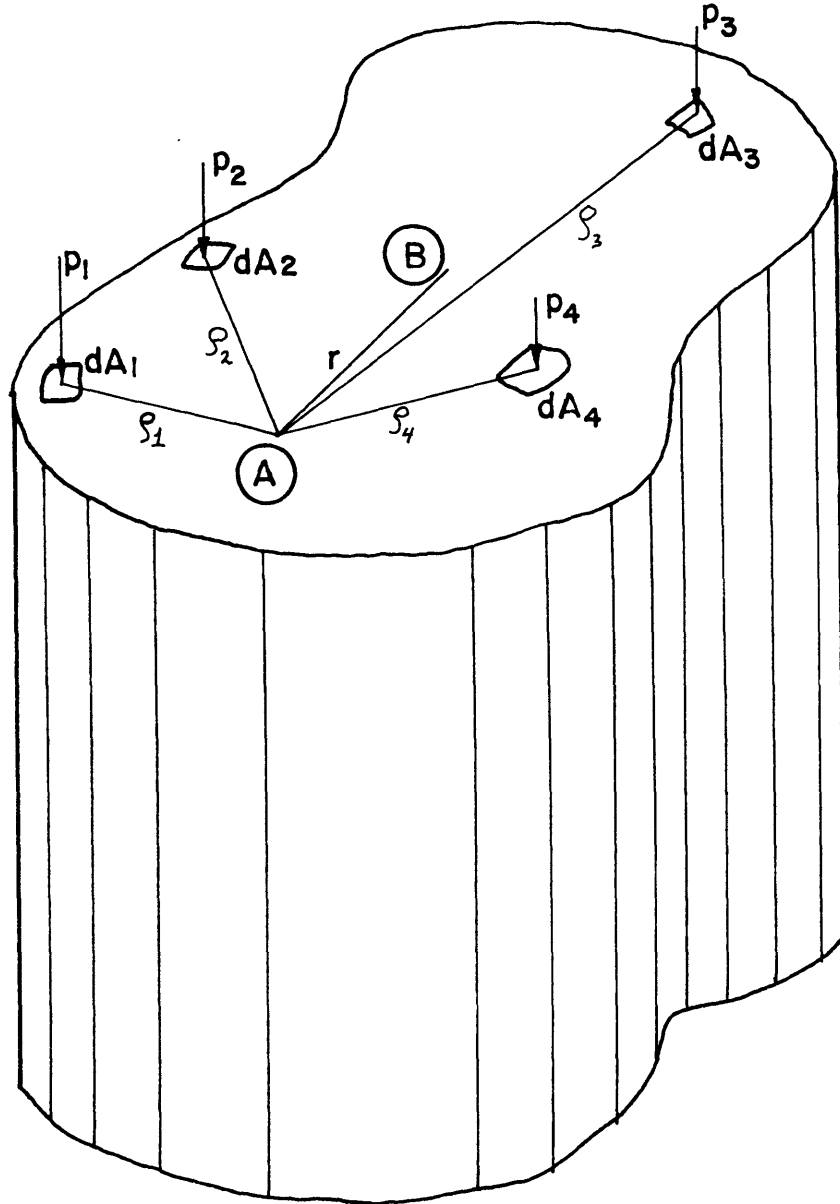


FIG. 5 TYPICAL CONTACT AREA

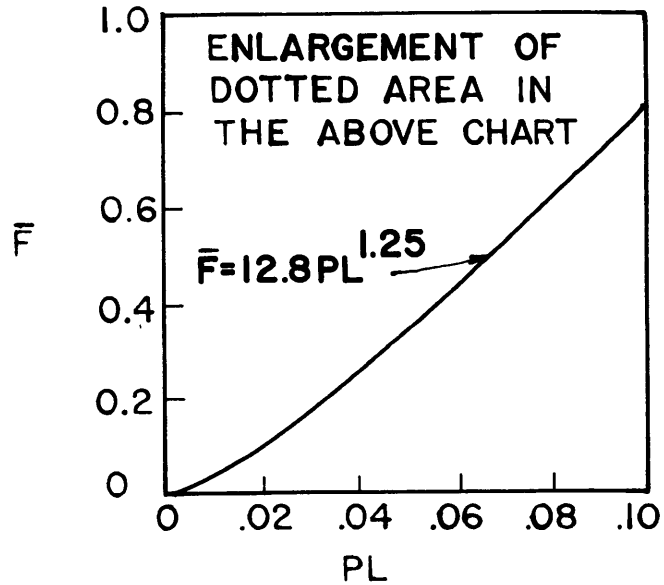
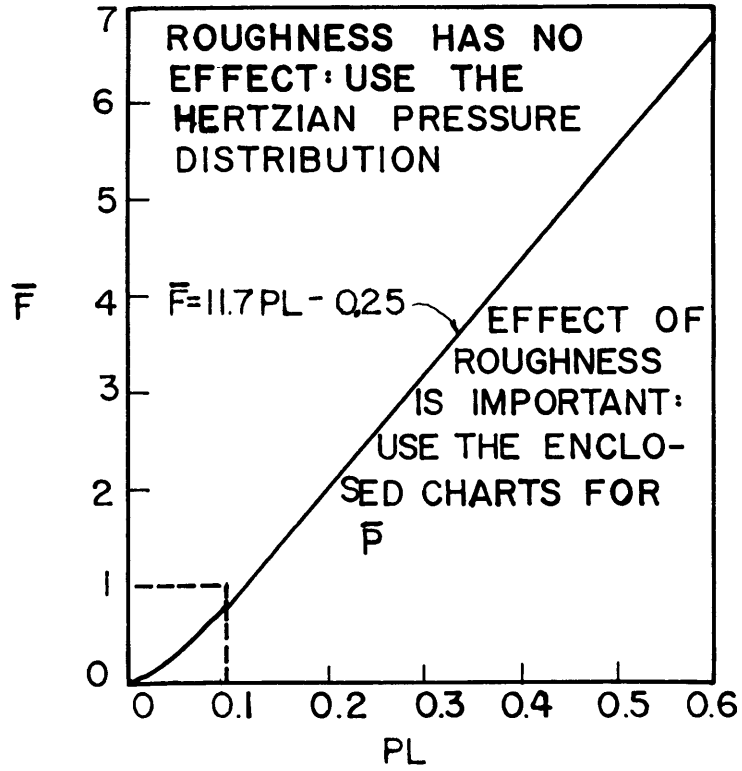


FIG. 6 REGION WHERE ROUGHNESS IS SIGNIFICANT

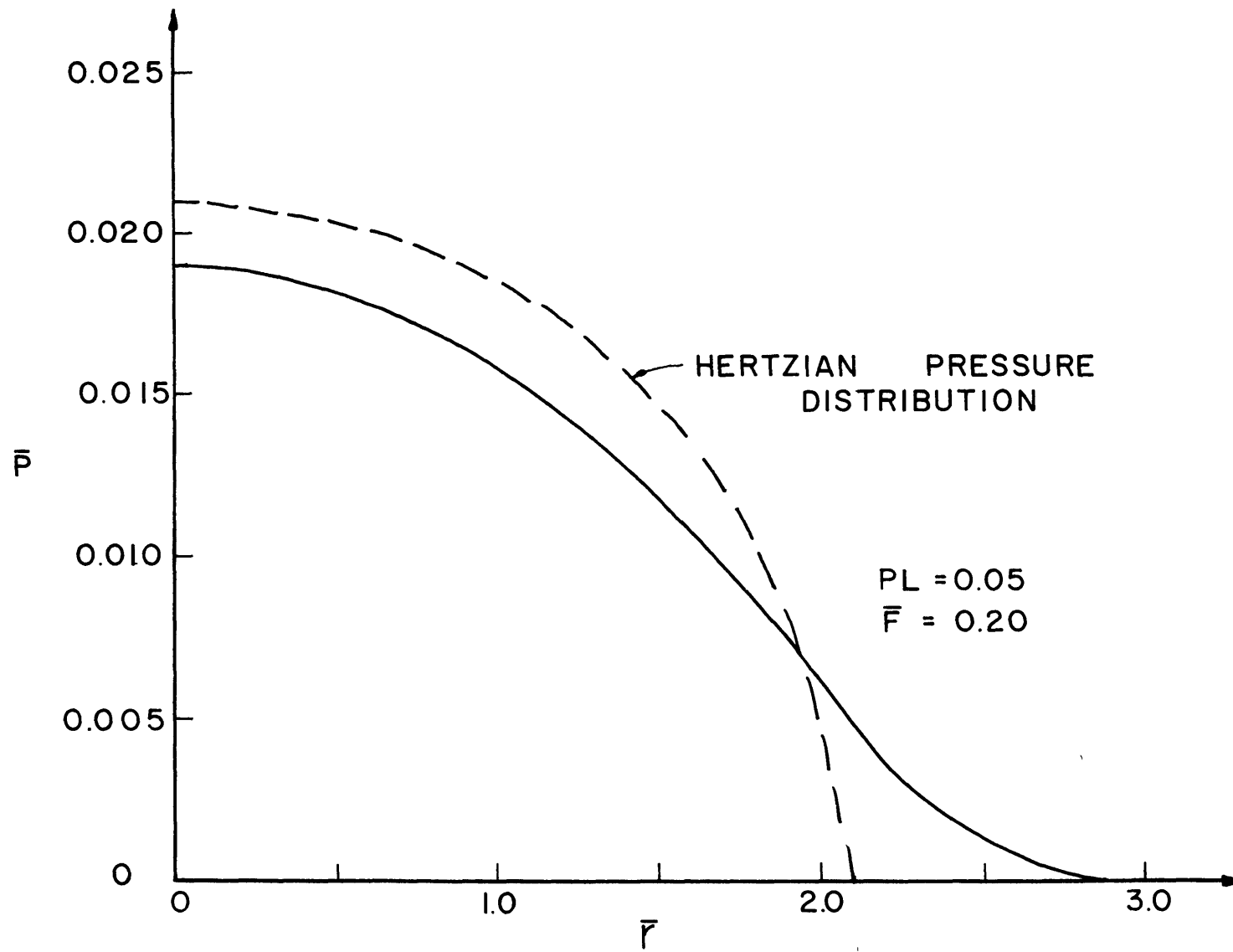


FIG. 7

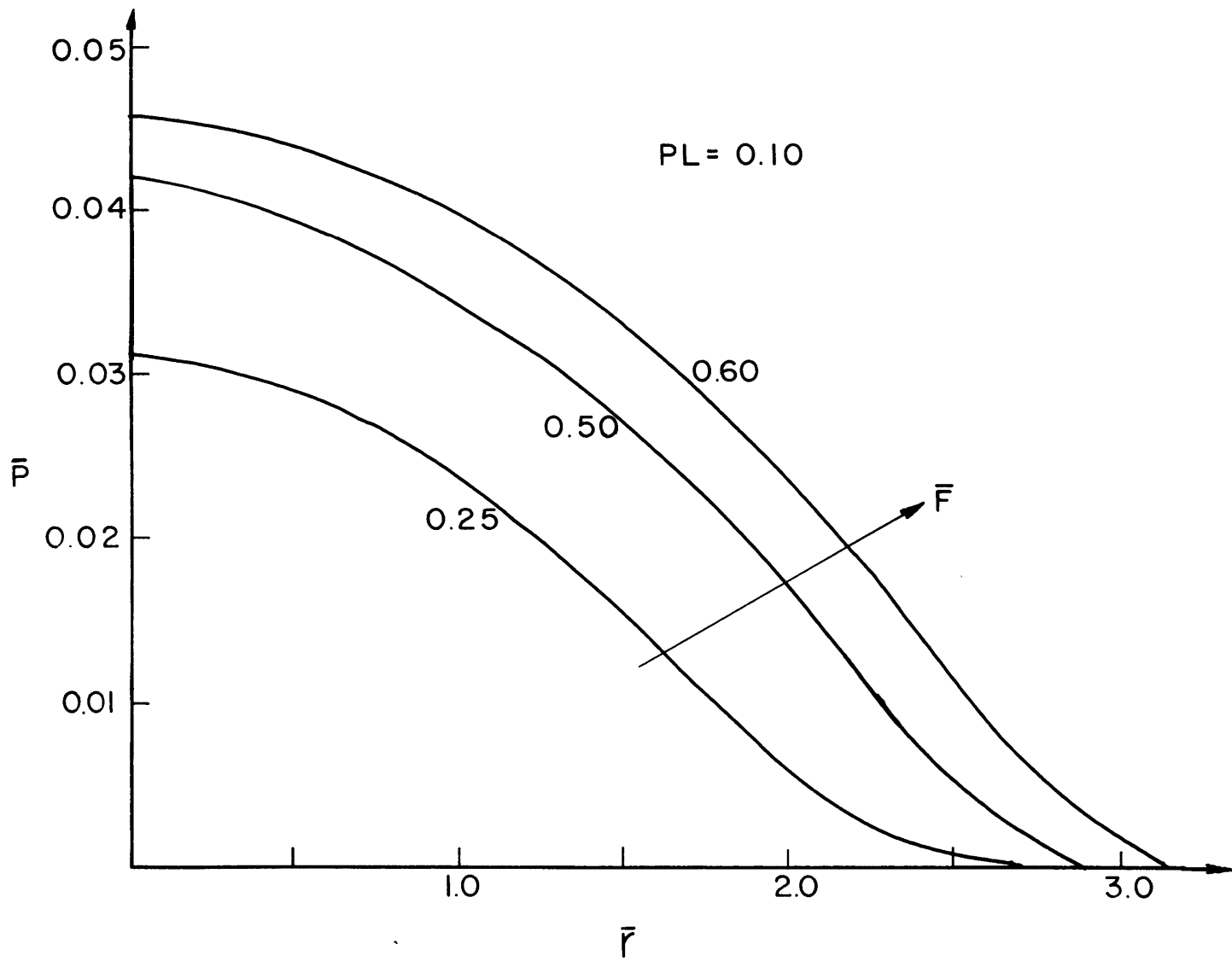


FIG. 8

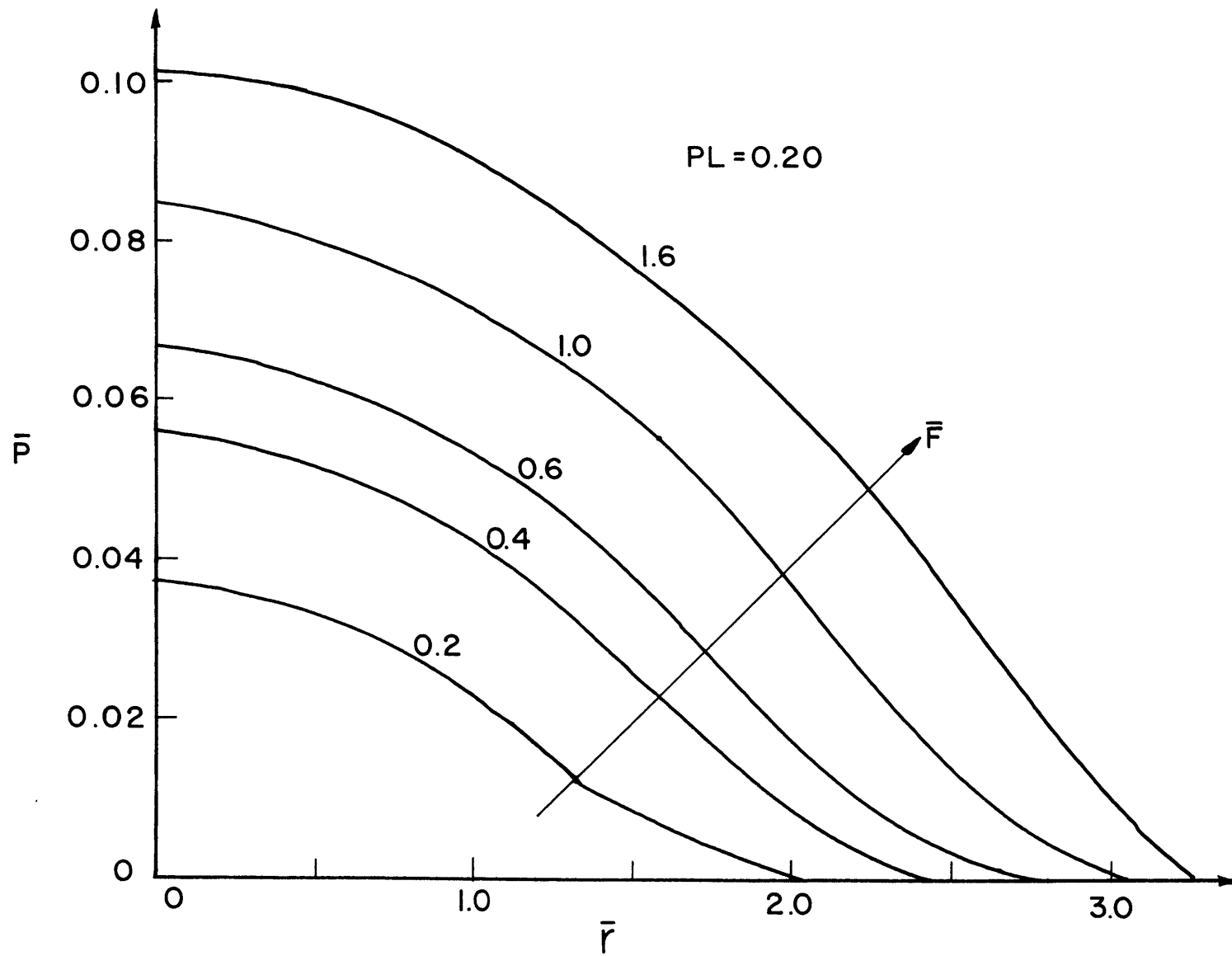


FIG. 9

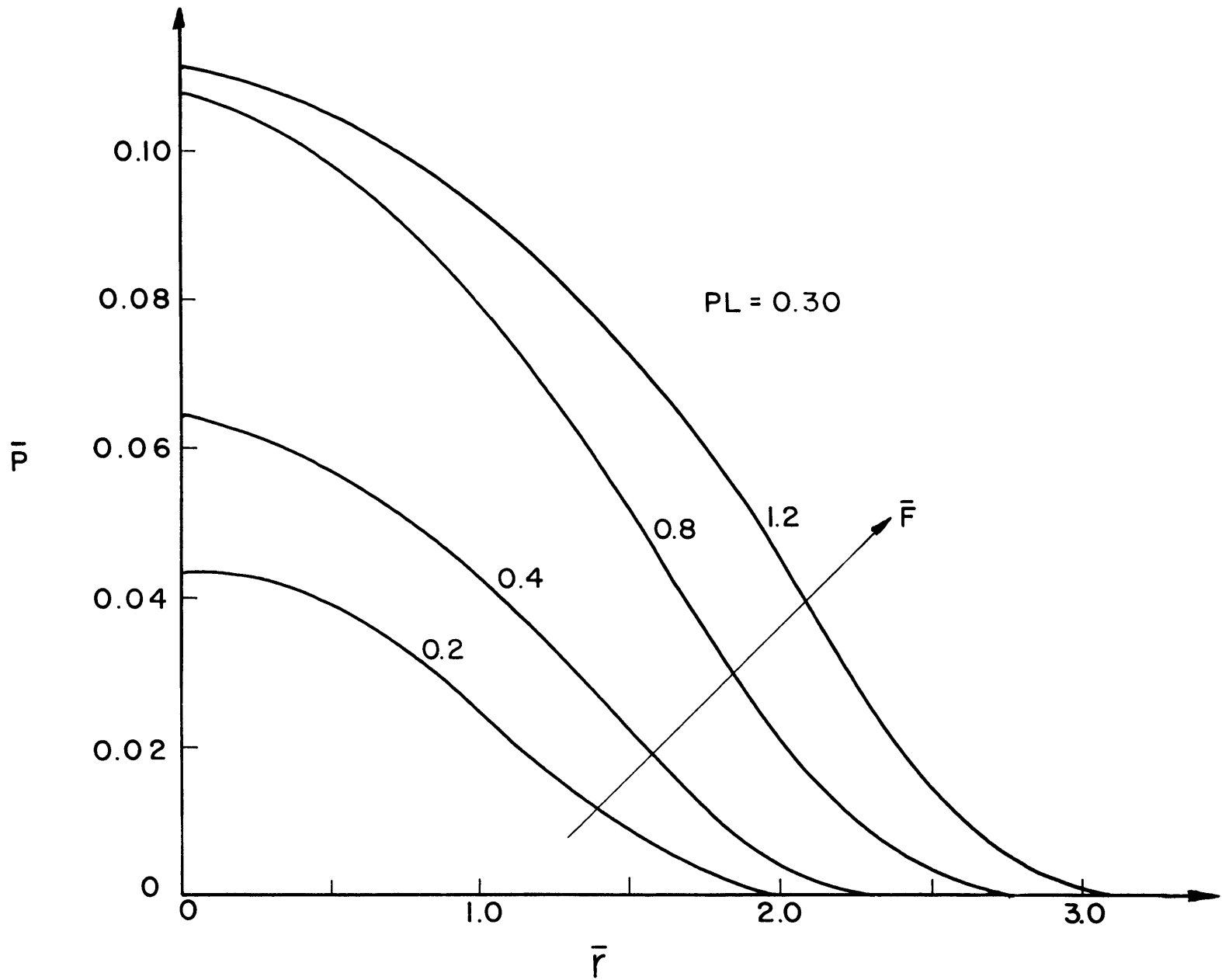


FIG. 10

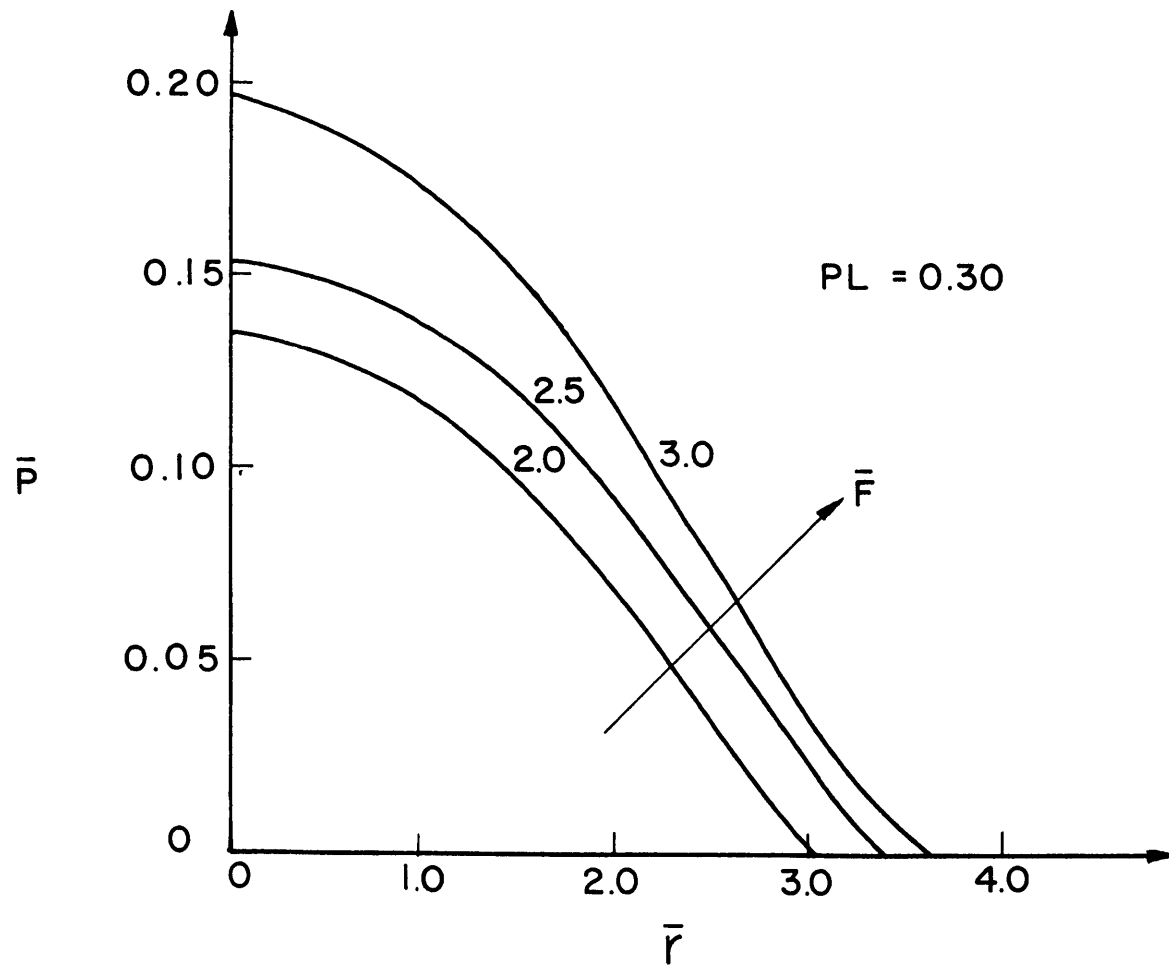


FIG. II

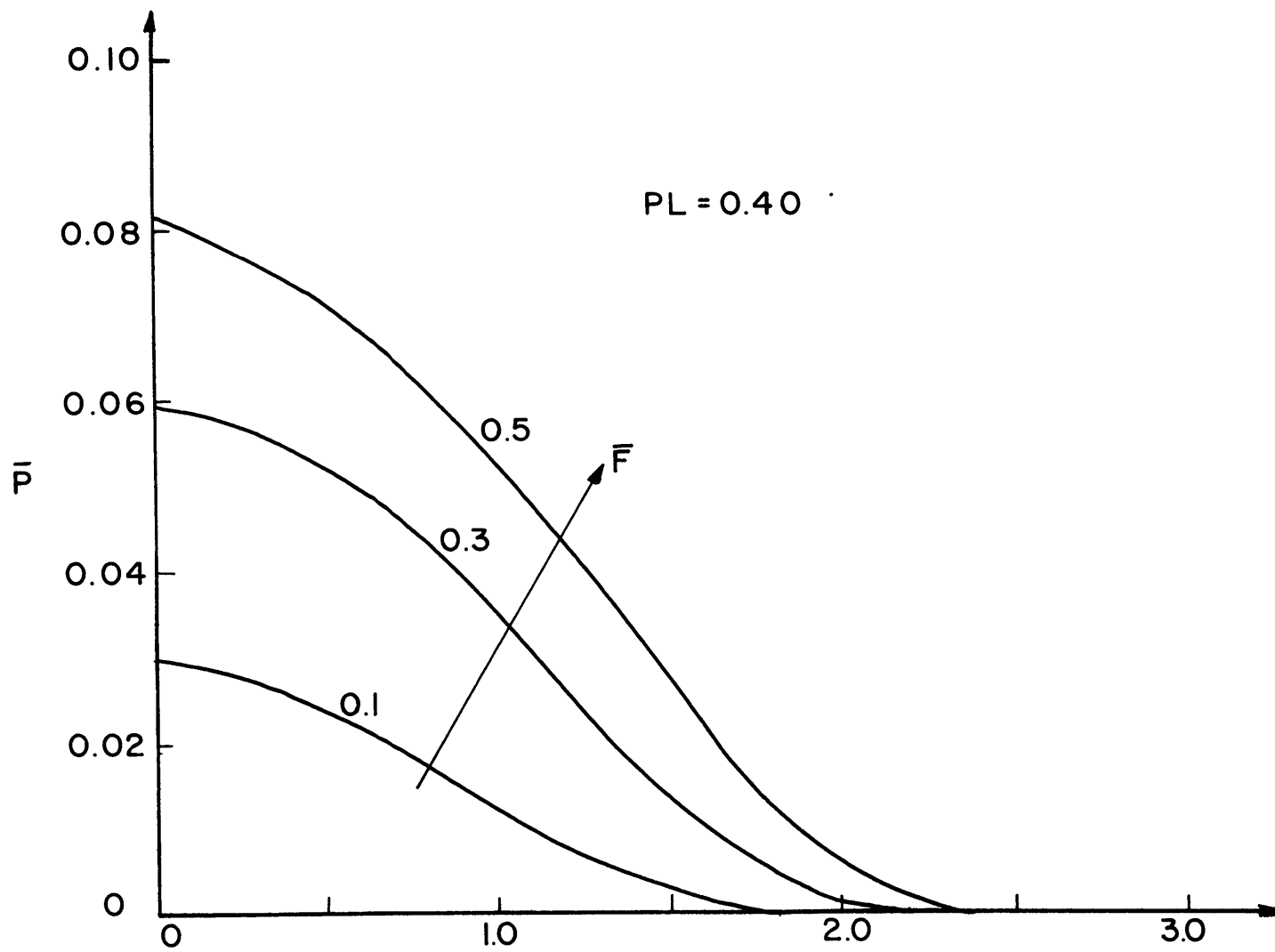


FIG. 12

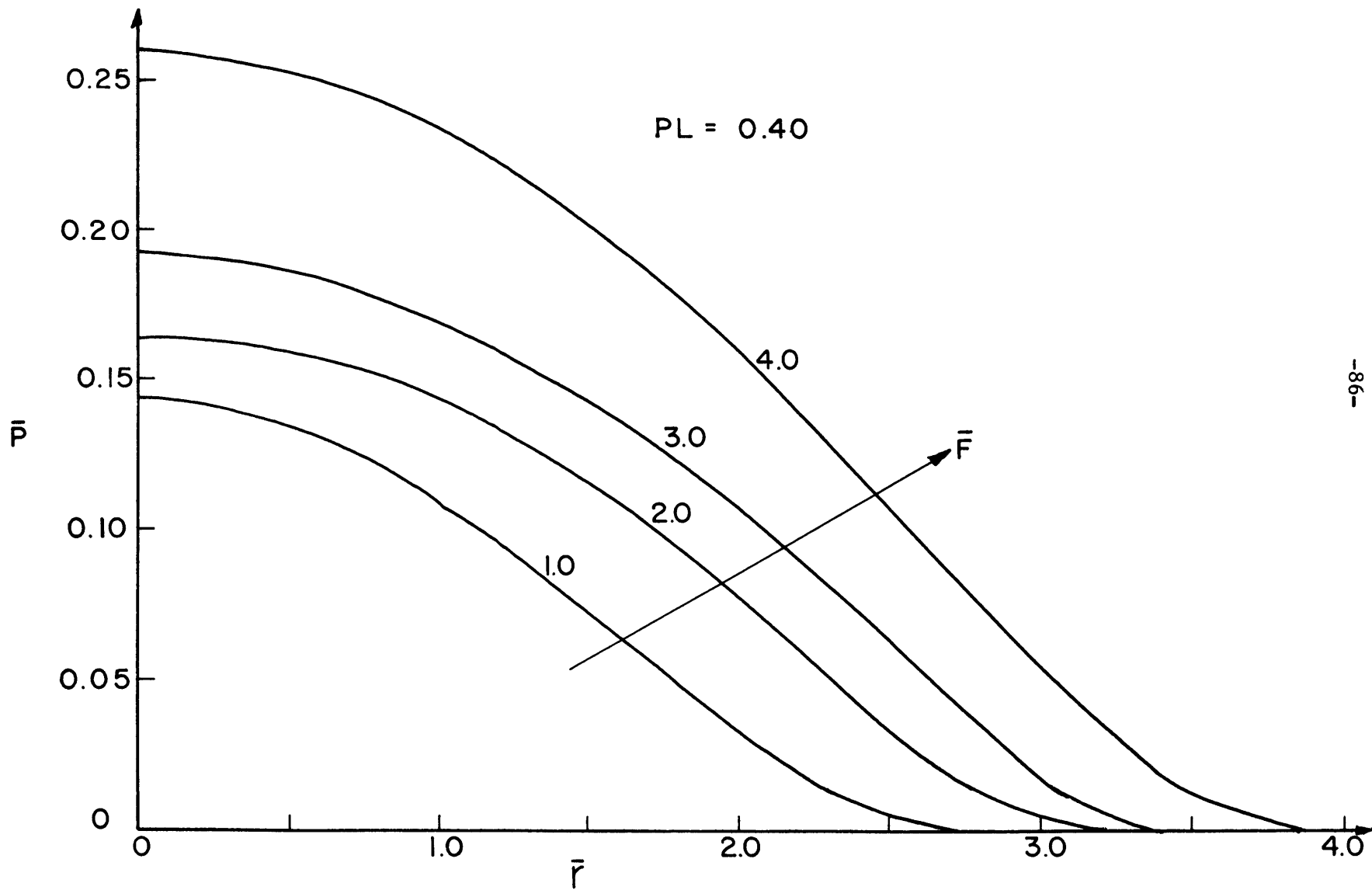


FIG. 13

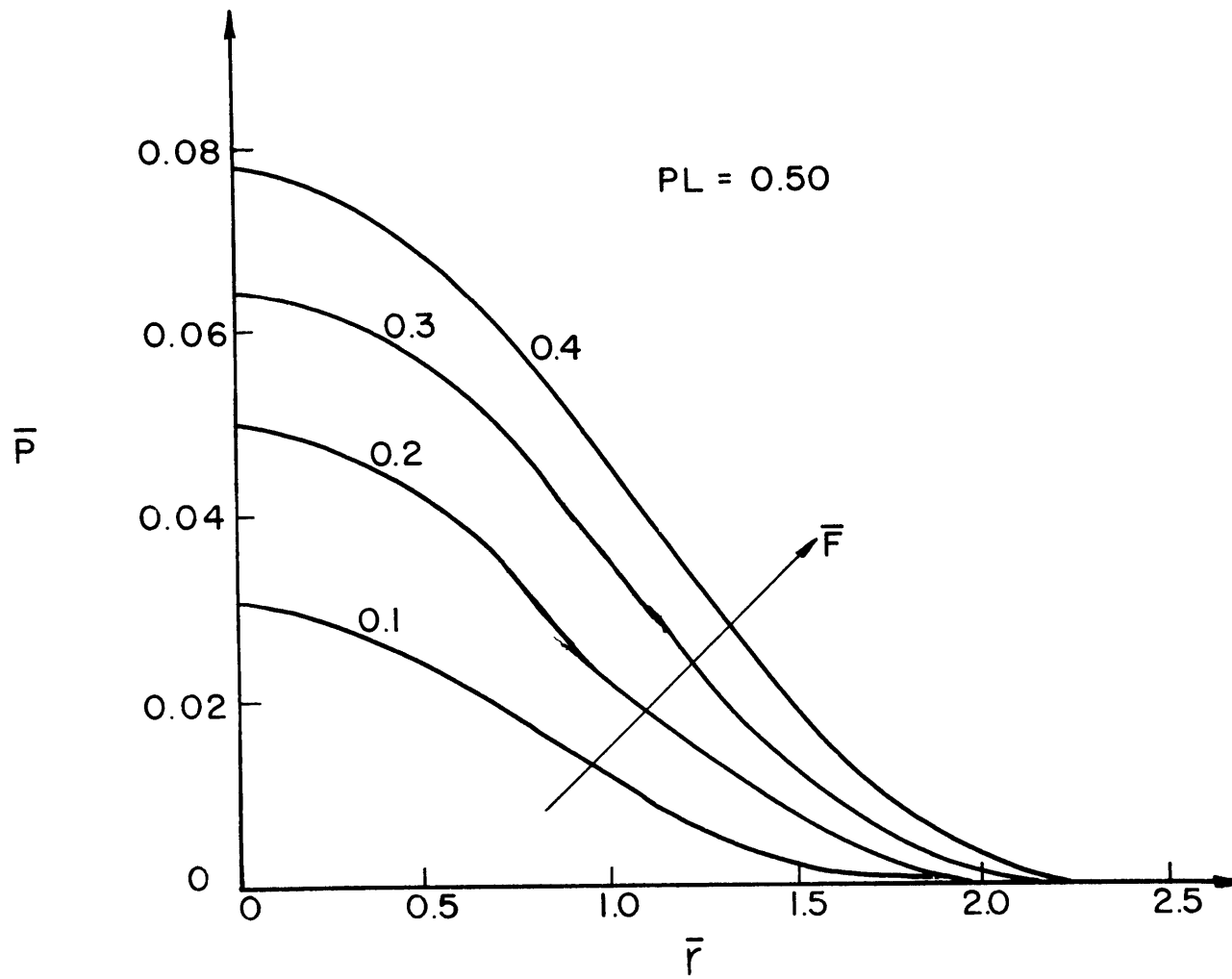


FIG. 14

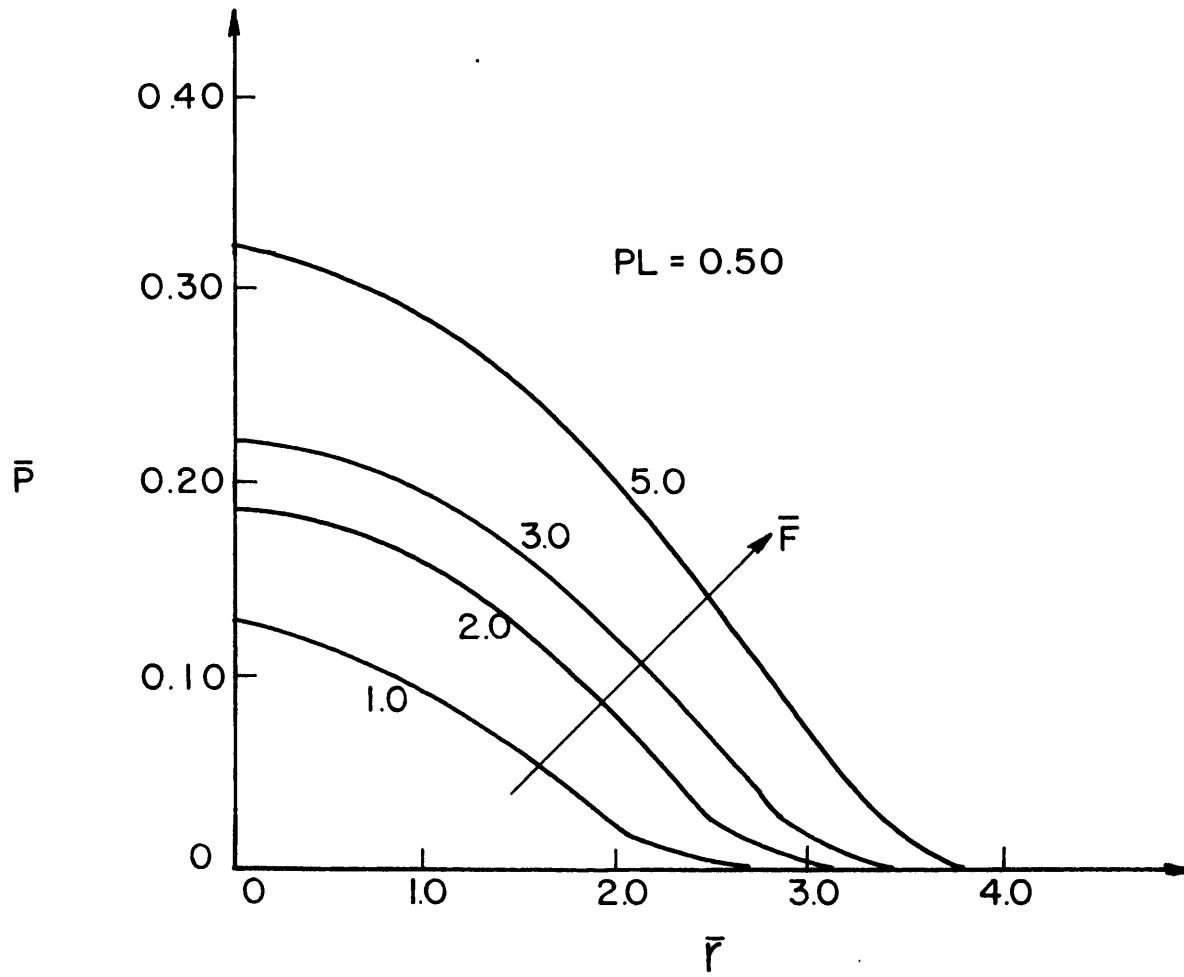


FIG. 15

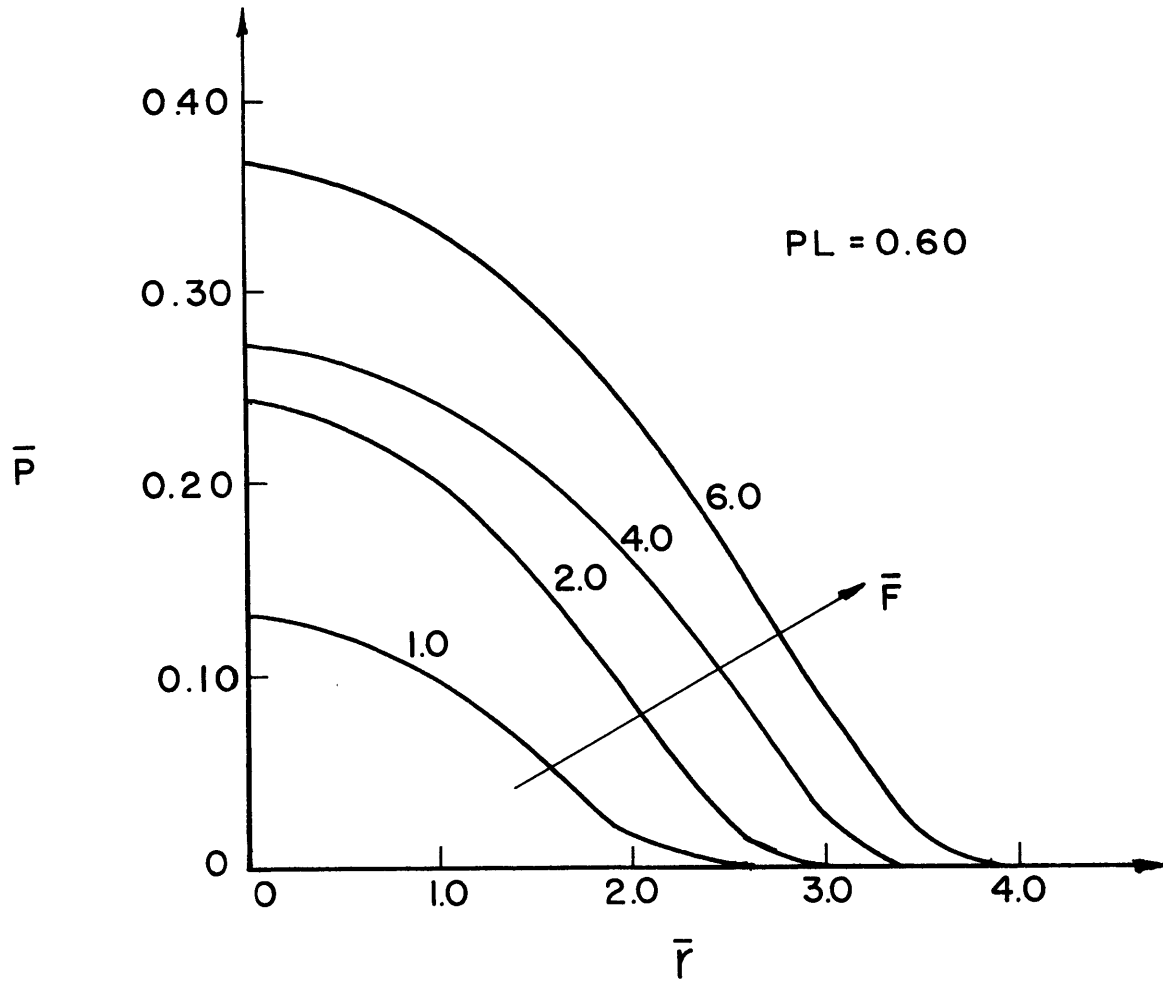


FIG. 16

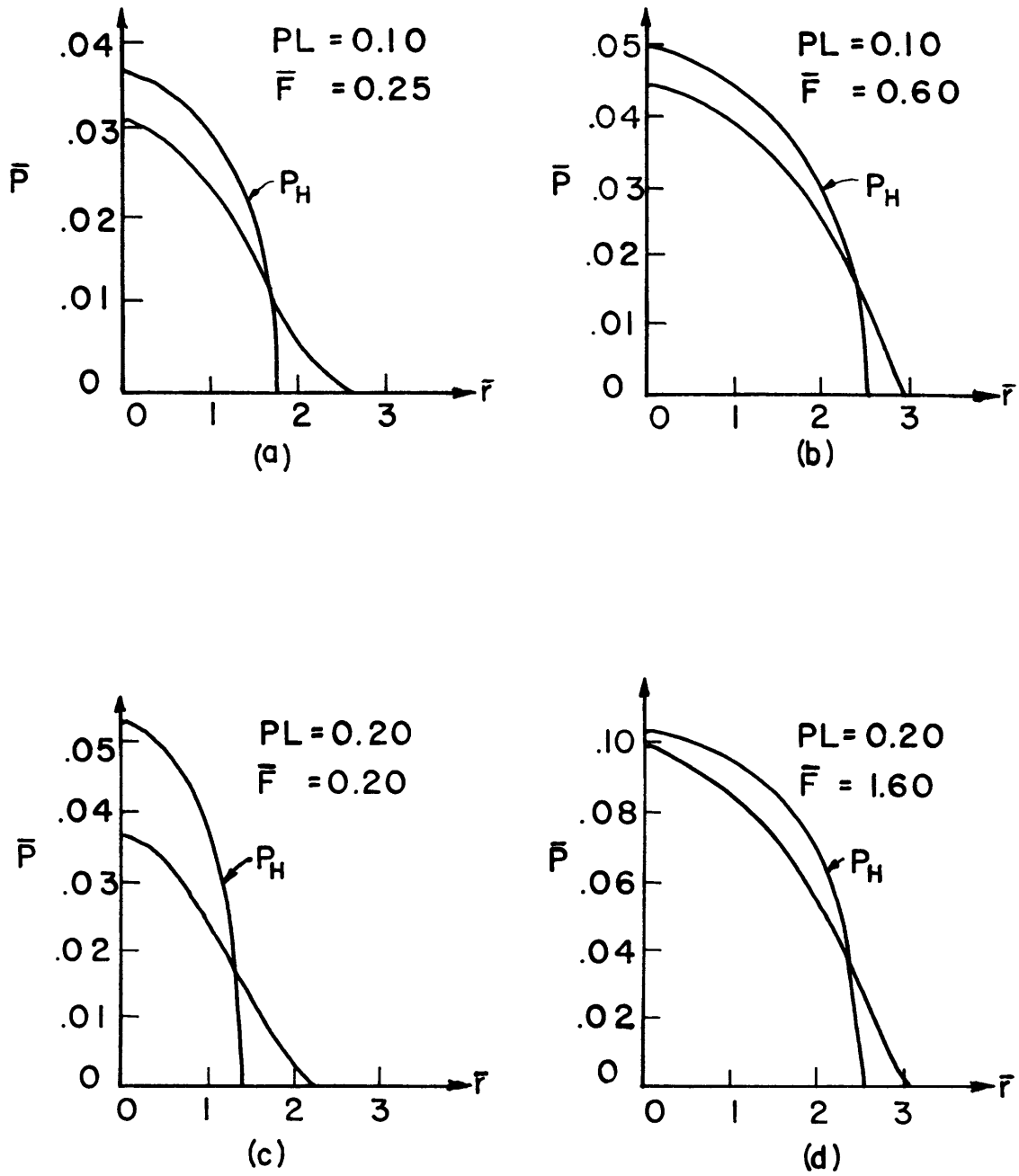


FIG. 17 COMPARISON OF HERTZIAN (P_H) AND ROUGH-SPHERE PRESSURE DISTRIBUTIONS

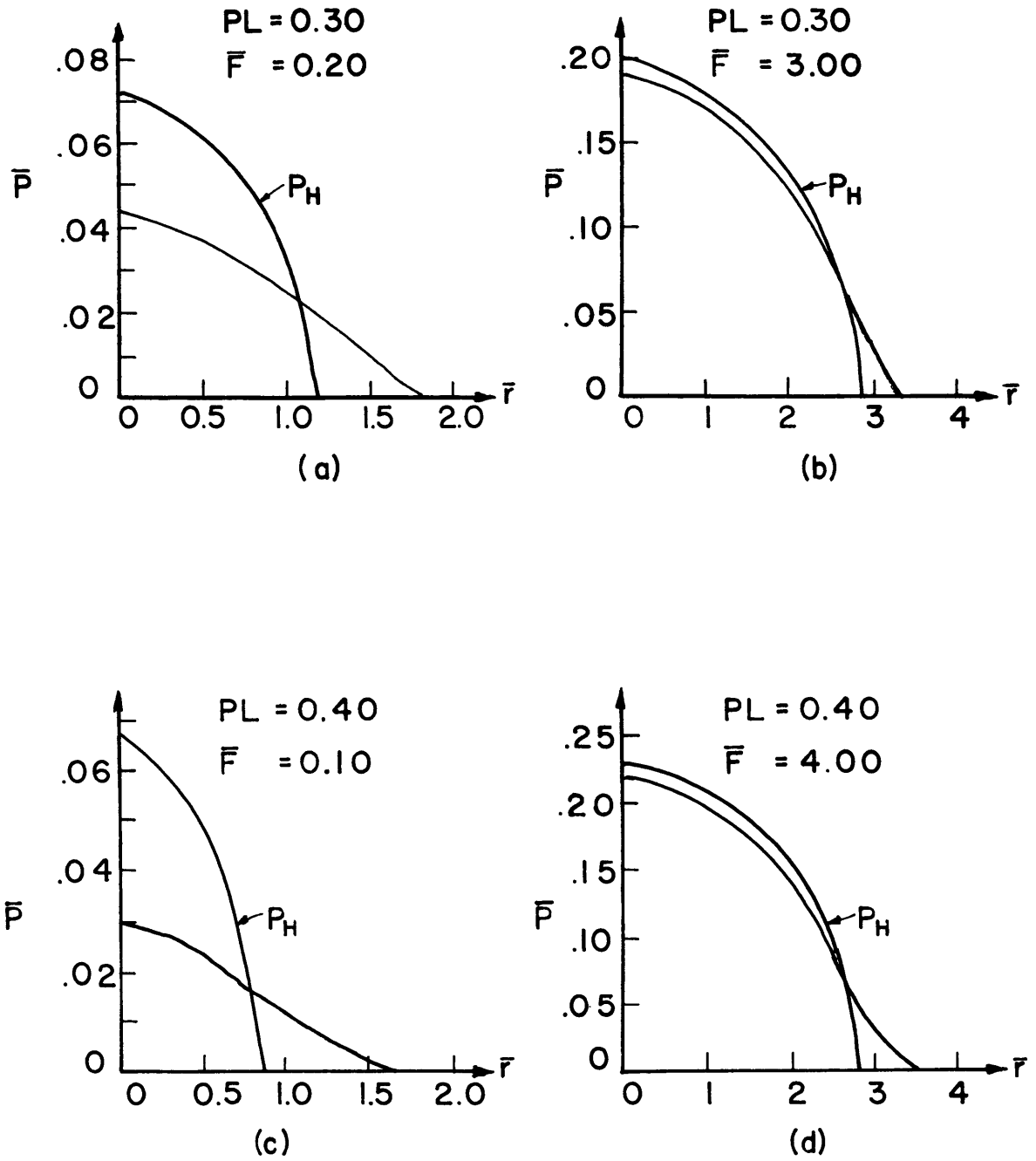
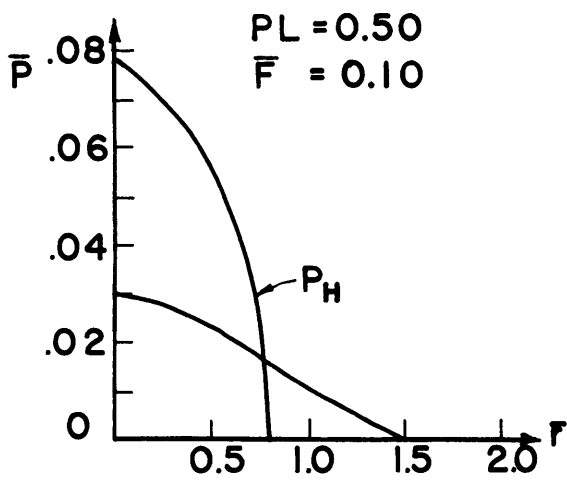
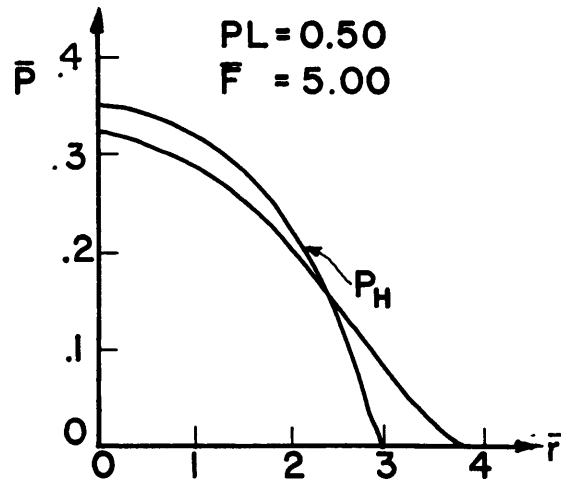


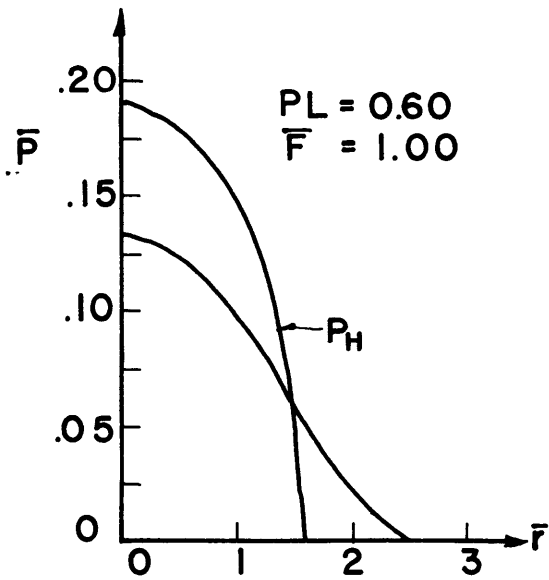
FIG. 18 COMPARISON OF HERTZIAN (P_H) AND ROUGH-SPHERE PRESSURE DISTRIBUTIONS



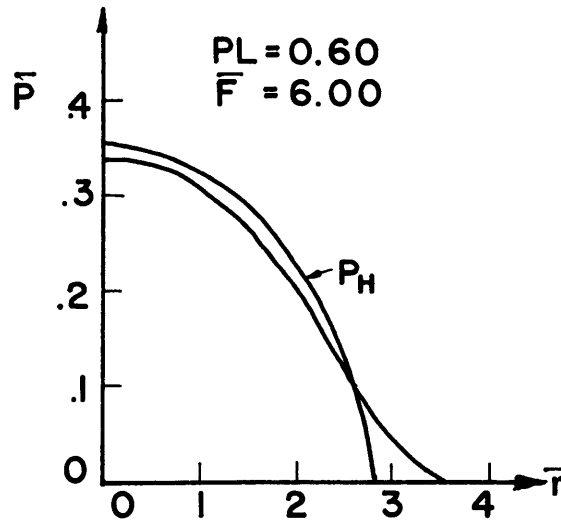
(a)



(b)



(c)



(d)

FIG. 19 COMPARISON OF HERTZIAN (P_H) AND ROUGH-SPHERE PRESSURE DISTRIBUTIONS

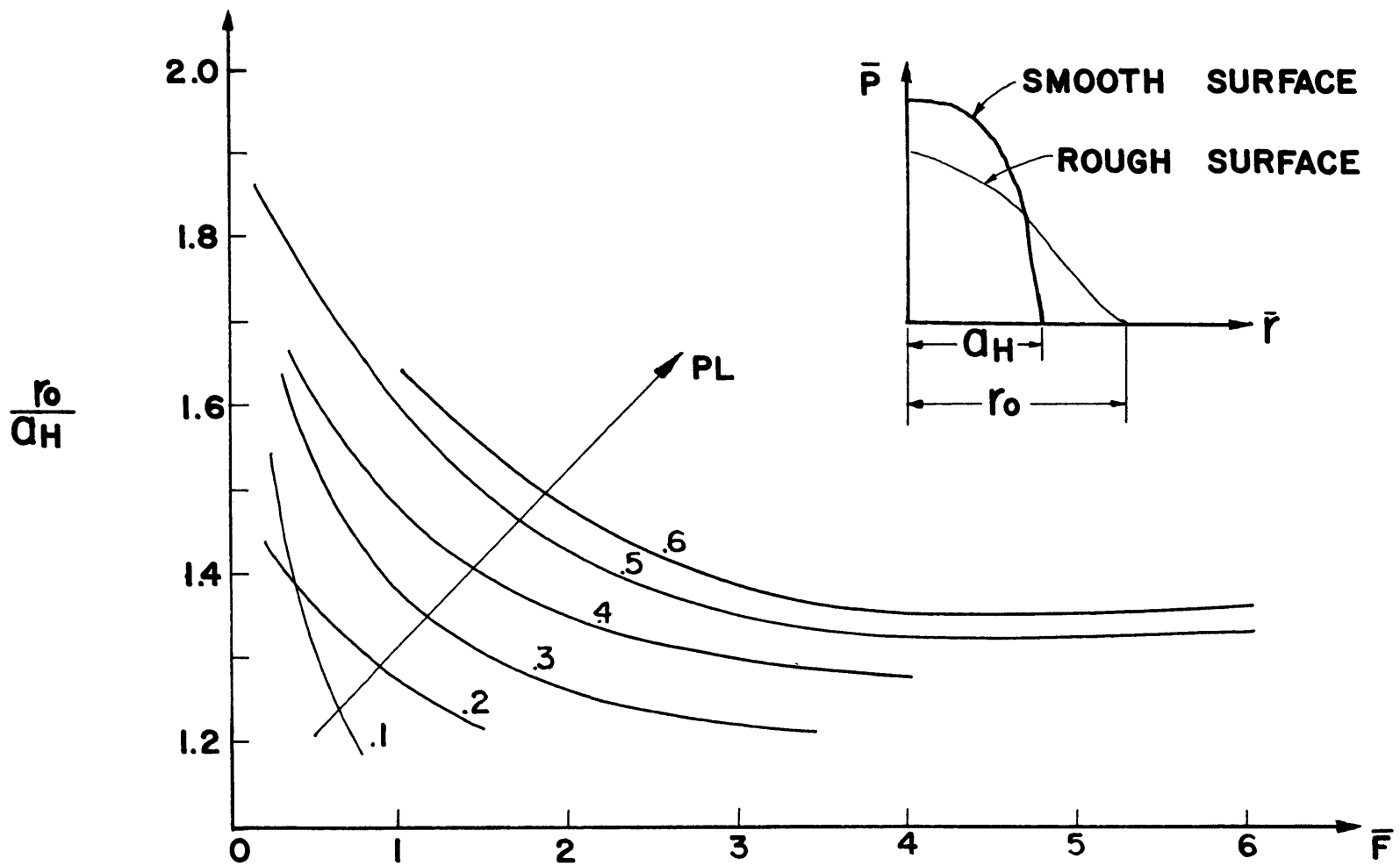


FIG. 20 RADIUS RATIO: SMOOTH VS. ROUGH SURFACES

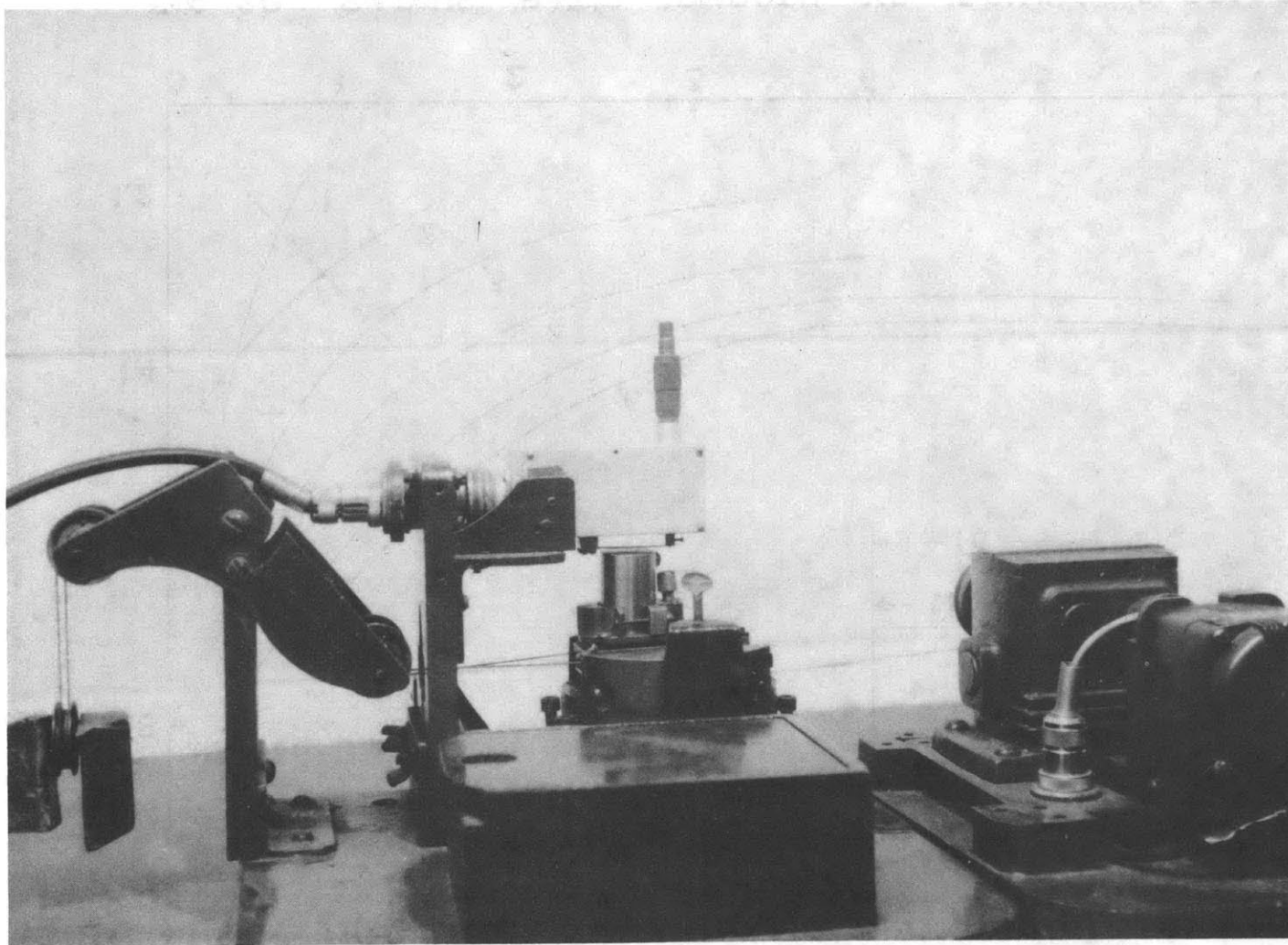


FIG. 21 SURFACE PROFILE MEASURING INSTRUMENT

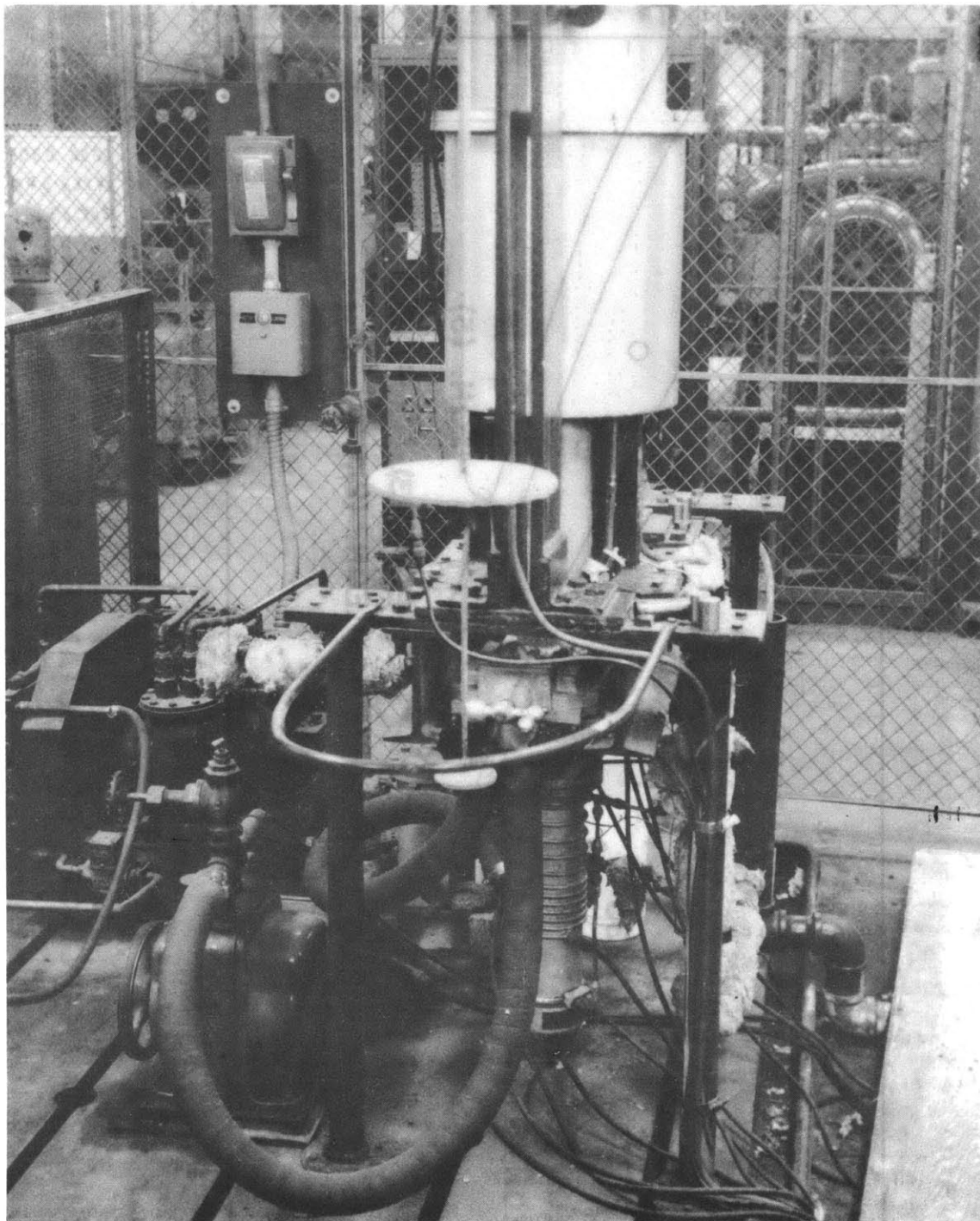


FIG. 22 CONTACT RESISTANCE APPARATUS

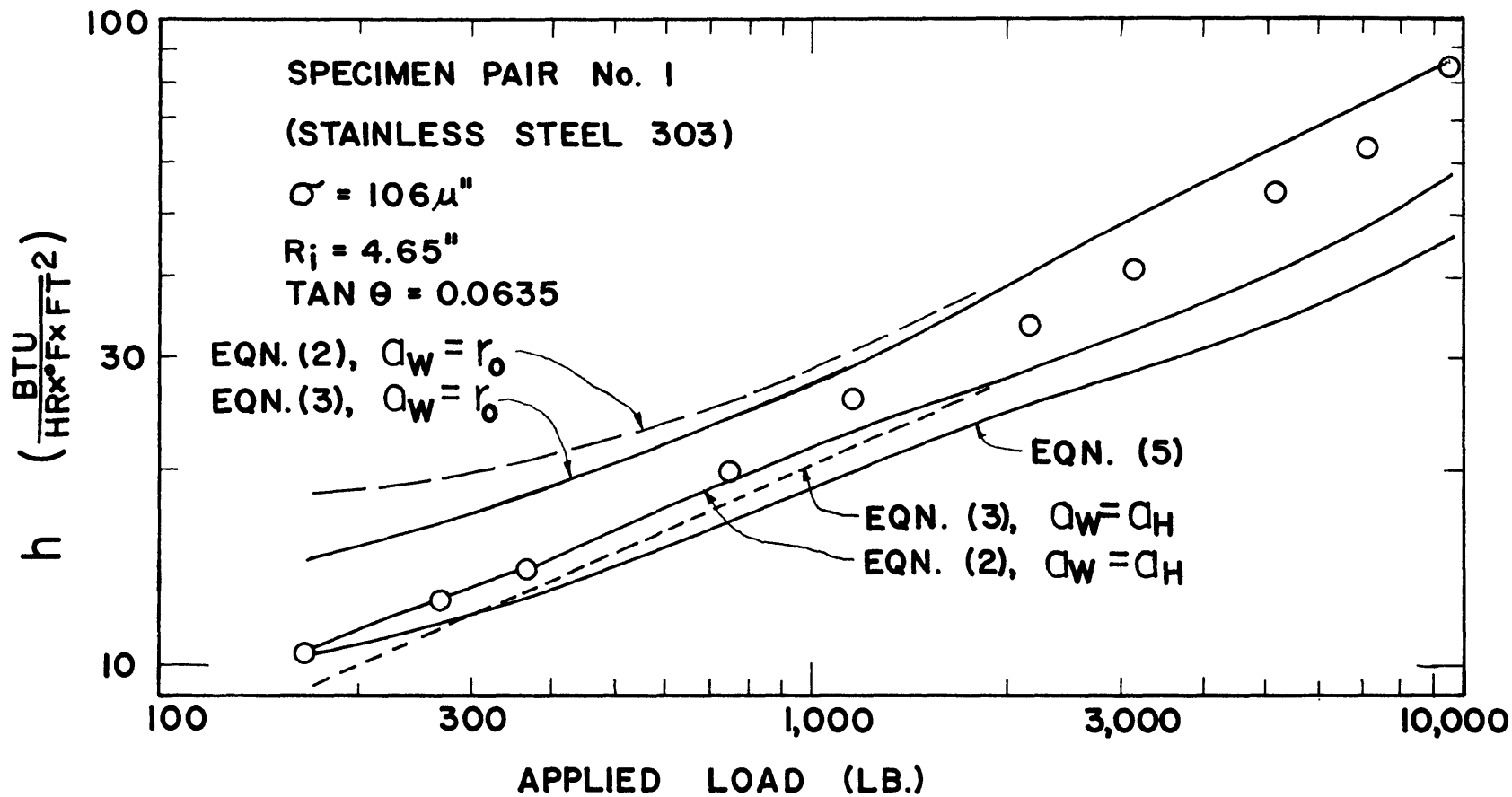


FIG. 23A. CONTACT CONDUCTANCE RESULTS

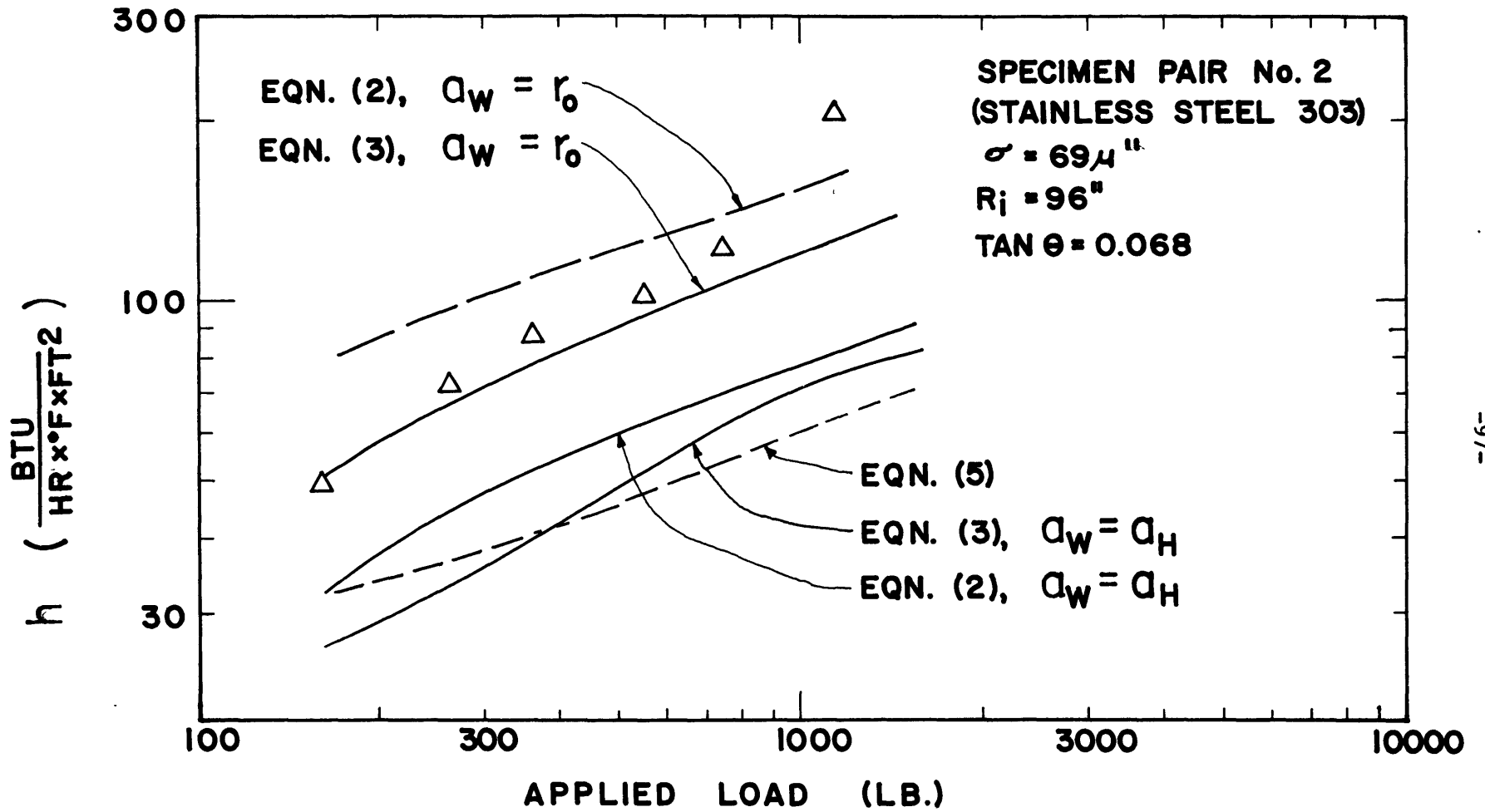


FIG. 23B. CONTACT CONDUCTANCE RESULTS

$T_0 =$ AMBIENT TEMPERATURE

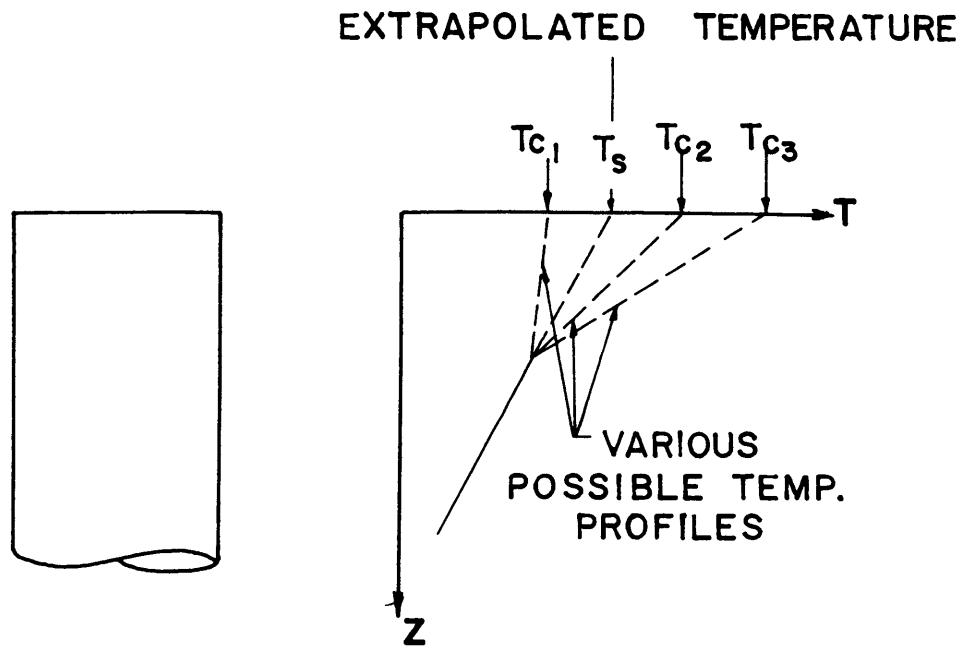
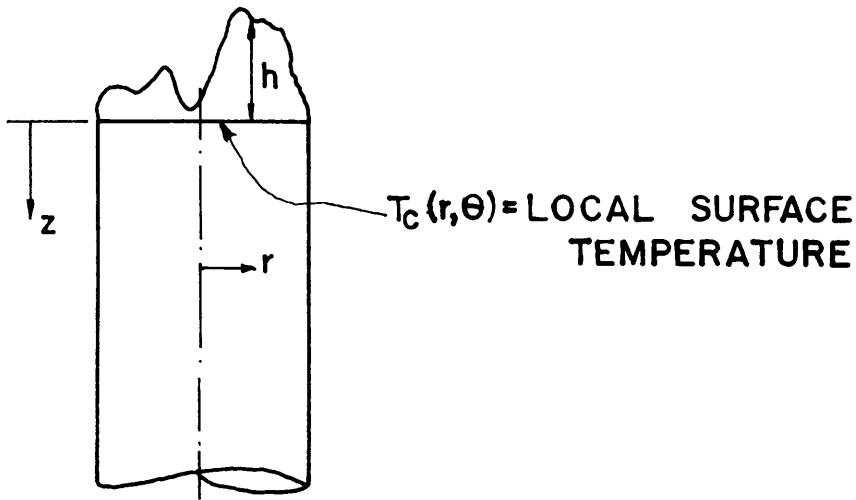


FIG. 24 NON - UNIFORM HEAT TRANSFER COEFFICIENT

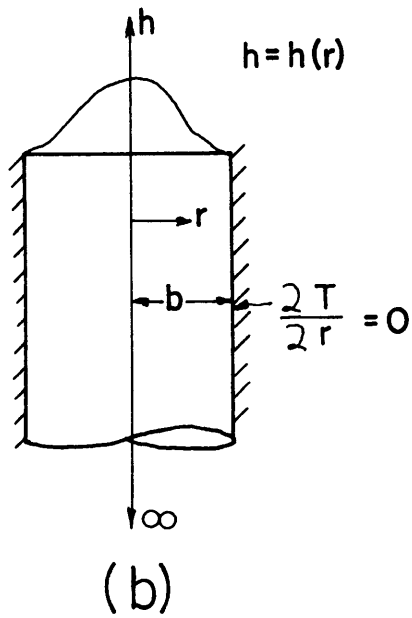
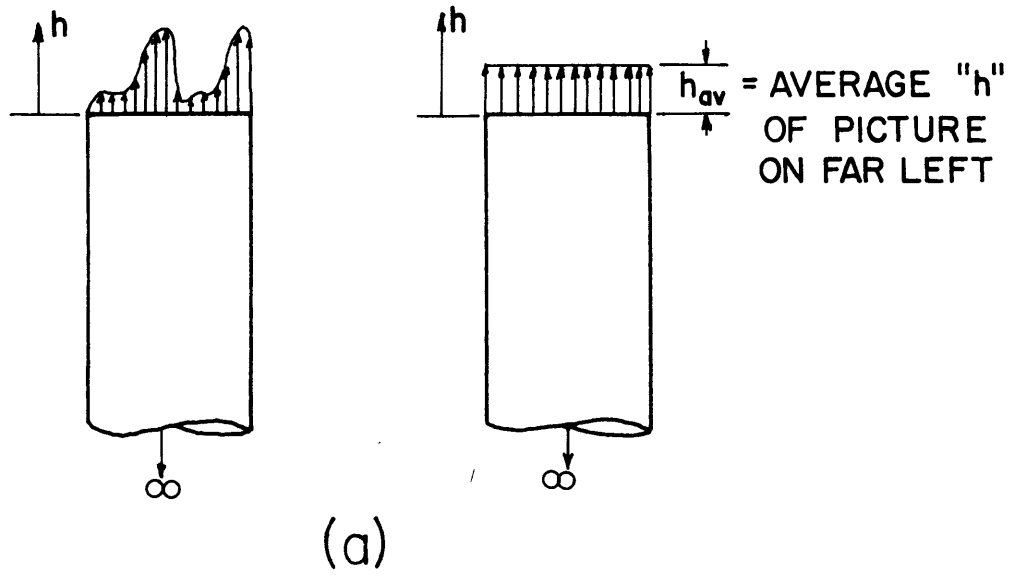


FIG. 25 NON - UNIFORM HEAT TRANSFER COEFFICIENT